X-735-69-25

NICKEL-CADMIUM BATTERY TEST PROJECT—RELATIONSHIP BETWEEN OPERATION, LIFE, AND FAILURE MECHANISM

Volume III. Analysis of the Cells and their Components

G. HALPERT

MARCH 1969

GSFC

GODDARD SPACE FLIGHT CENTER
GREENBELT, MARYLAND

X-735-69-25

NICKEL-CADMIUM BATTERY TEST PROJECT— RELATIONSHIP BETWEEN OPERATION, LIFE, AND FAILURE MECHANISM

VOLUME III. ANALYSIS OF THE CELLS AND THEIR COMPONENTS

G. Halpert
Materials Research and Development Branch
Systems Division

March 1969

GODDARD SPACE FLIGHT CENTER
Greenbelt, Maryland

NICKEL-CADMIUM BATTERY TEST PROJECT—

RELATIONSHIP BETWEEN OPERATION, LIFE,

AND FAILURE MECHANISM

VOLUME III. ANALYSIS OF THE CELLS AND THEIR COMPONENTS

G. Halpert
Materials Research and Development Branch
Systems Division

ABSTRACT

Nickel-cadmium aerospace batteries were operated in different but related cycling schemes at the Baltimore Division of the Aerospace Group, Martin Marietta Corporation, in an effort to relate cycle life to method of operation (see Vols. I and II on this subject). When five of the ten cells in a battery "failed," the remaining "active" cells were removed from test, the cell cans were opened, and the plates and separators were analyzed. The objective in performing a physical-chemical analysis on the cell materials was to determine what the long-term degradation processes were and whether they could be related to a specific type of operation. Visual examination, wet chemical techniques, instrumental methods, and cell overdischarge and oxygen recombination tests employed in the analysis of the materials are described in this report. The results indicate that, although there is wide variation in the materials, there was a general long-term mode of degradation common to all batteries regardless of operational scheme. The mechanism of failure involved the migration of electrolyte into the plates, the consequent drying-out of the separator, and the growth of negative active material through the separator—the last-named process resulting in strong adhesion of the separator to the negative plates. Specific characteristics of the materials found from measurements of pore size distribution, surface area, crystal structure, spectrochemical analysis, differential thermal analysis, and oxygen recombination rates are all discussed in this report.

CONTENTS

CONTENTS (Continued)

ILLUSTRATIONS

TABLES

TABLES (Continued)

NICKEL-CADMIUM BATTERY TEST PROJECT—

RELATIONSHIP BETWEEN OPERATION, LIFE,

AND FAILURE MECHANISM

VOLUME III. ANALYSIS OF THE CELLS AND THEIR COMPONENTS

INTRODUCTION

This report describes the results of the physical, chemical, and electrochemical tests on cells in the Nickel-Cadmium Battery Test Project that were performed at the Baltimore Division of the Aerospace Group, Martin Marietta Corporation, under Contract NAS-5-3027. It is the fourth report in the series concerning the battery test program, in which 15 batteries were cycled under different but related operating conditions in an effort to establish relationships between mode of operation and cycle life.

The reporting of this nickel-cadmium battery test project, including the experimental design, battery cycling test, computer programs, and the analysis of the cells, has been divided into four reports. The experimental plan and program outline for the overall project are given in the first volume (Reference 1). The second report, or Volume II (Reference 2), includes a description of the battery cycling test, the results achieved, and the relationships derived between operation and cycle life. The third report (Reference 3) of the series presents a set of computer programs with operating instructions for use in abstracting, computing, and presenting battery test data.

In this—the fourth—report (Volume III*), the results of the physical, chemical, and electrochemical investigation of the cell and its components are given. This analysis phase of the battery test program was not included in the original program plan. The analysis of the cells and their component materials was, however, a logical extension to such a program. It was expected that these tests would give insight into the causes of long-term degradative processes occurring in these cells and relate these degradative processes to the type of operation to which the cells had been subjected.

*The third report is not designated as a volume.

ANALYSIS TEST PROGRAM

This phase of the program commenced when a battery was considered to have "failed" (five failed cells* constituted battery failure). The five remaining "active" cells were cycled again for a short time, using the same operational scheme, and then subjected to a set of physical-chemical test experiments. The batteries from which the test cells were removed are those which were used in the battery test cycling program described in Figure 1.

The test program to analyze the components followed the sequence outlined in Figure 2. The five "live" cells were designated A through E for each battery. The electrodes (plates) of cells A and B were separately numbered. The designations A-1, A-2, etc., refer to the positive and negative plates in a cell (A-1 refers to the outside negative plate of cell A). Odd numbers were given to the negative plates, even numbers to the positives. The cells in the test program were Gulton VO-6HS type which contained ten (10) cadmium-hydroxide-filled sintered plate negatives and nine (9) nickel-hydroxide-filled sintered plate positives. The plates were constructed using the SAFT process of sintered carbonyl powder nickel on a perforated nickel-plated steel base. The separation between plates was maintained with a non-woven nylon separator.

When the battery failed, the "live" test cells were immediately removed from the chamber in which they were cycling. Cells A and B were shipped to Gulton Industries, Inc., Metuchen, N. J., for the component analysis. There the cells were opened within a six-hour period in order to minimize the effects due to inactivity. Cells C, D, and E were put into a test program at Martin Marietta Corporation, Baltimore, Md., to determine the cell character after the long-term cycling test.

Upon arrival at Gulton, cells A and B were opened on a milling machine covered with a plastic bag through which argon was circulated. The cell components were immediately placed into sealed containers and transferred to a controlled-atmosphere chamber. The plates were designated A-1 through A-19 and B-1 through B-19. After weighing, plates numbered B-1 through B-10 were placed into individual sealed containers which in turn were placed into a single sealed jar for shipment to the ESB Inc. Research Center at Yardley, Pennsylvania. Upon arrival the jar was immersed, opened, and washed in oxygen-free distilled water. The plates were dried in an oven at 45° C overnight, cooled in a desiccator, and weighed. The remaining plates at

*A failed cell was one in which (1) the discharge voltage had fallen below 1.0v before completion of the normal discharge half-cycle, or (2) the voltage had exceeded 1.50v during the normal charge half-cycle, or (3) a loss of more than 75% of its initial capacity had occurred.

GROUP I	GROUP II	GROUP III	GROUP IV	GROUP V
START PROGRAM WITH CELLS FULLY CHARGED			FULLY DISCHARGED	FULLY CHARGED
BATTERY 0	BATTERY 3 - 25% DOD	BATTERY 7 - 100% OVERCHARGE	BATTERY 10 - 50% HOC	PACK 13 NAD-CRANE - 25% DOD
CHARGE - C/10 FOR 3-1/4 HR DISCHARGE - C/2 FOR 1/2 HR	CHARGE - C/10 TO E_T DISCHARGE - C/2 FOR 1/2 HR	CHARGE - C/10 FOR 6-1/2 HR DISCHARGE - C/2 FOR 1/2 HR	CHARGE - C/5 FOR 2-1/2 HR DISCHARGE - C/2 TO 1 0V	CHARGE 1 875 AMPS FOR 1 HR DISCHARGE 3 0 AMPS FOR 1/2 HR
BATTERY 1 - SLOW DISCHARGE	BATTERY 4 - 25% DOD	BATTERY 8 - CONSTANT V	BATTERY 11 - 50% HOC	PACK 17 NAD-CRANE -25% DOD
CHARGE - C/10 FOR 3-1/4 HR DISCHARGE - C/8 FOR 2 0 HR	CHARGE - C/5 TO E_T THEN C/10 TO E_T DISCHARGE - C/2 FOR 1/2 HR	CHARGE - CONSTANT V TO C/10 DISCHARGE - C/2 FOR 1/2 HR	CHARGE - C/2 FOR 1 HR DISCHARGE - C/2 TO 1 0V	CHARGE 0 75 AMP FOR 2-1/2 HR DISCHARGE 3 0 AMPS FOR 1/2 HR
BATTERY 2 - RAPID DISCHARGE	(3A) BATTERY 12 - 25% DOD	BATTERY 9 - PRESS TERM		
CHARGE - C/10 FOR 3-1/4 HR DISCHARGE - 2C FOR 1/8 HR	CHARGE - C/5 TO 1 425V DISCHARGE - C/2 FOR 1/2 HR	CHARGE - C/10 TO PRESS CUTOFF DISCHARGE - C/2 FOR 1/2 HR		
	(5A) BATTERY 13 - 25% DOD		AMF CYCLE (INCLUDES AMF 25° PLUS AMF 10° AND 40°)-UDC - 58% DOD	
	CHARGE - C/2 TO 1 450V DISCHARGE - C/2 FOR 1/2 HR			
	(6A) BATTERY 14 - 25% DOD		CHARGE - CONSTANT V 65 MIN DISCHARGE - LOAD - 6 AMP -35 MIN (Every 4th cycle drain through 0 5 - ohm resistor for 1 67 hours)	
	CHARGE - C/2 FOR 10 MIN THEN C/10 TO 1 42V DISCHARGE - C/2 FOR 1/2 HR			

BATTERY 5 - 50% DOD	BATTERY 6 - 100% DOD
CHARGE - C/2 TO E_T THEN C/10 TO E_T DISCHARGE - C/2 FOR 1 HR	CHARGE - C/2 TO E_T THEN C/10 AMPS TO E_T DISCHARGE - C/2 TO 1 0V

KEY C refers to the average cell capacity, not nominal capacity The C/10 rate is therefore 0 63 amp E_T is the end-of-charge voltage of Battery 0

DOD = depth of discharge
HOC = height of charge

Figure 1. Battery Test Program (6-ampere-hour cells at 25° C)

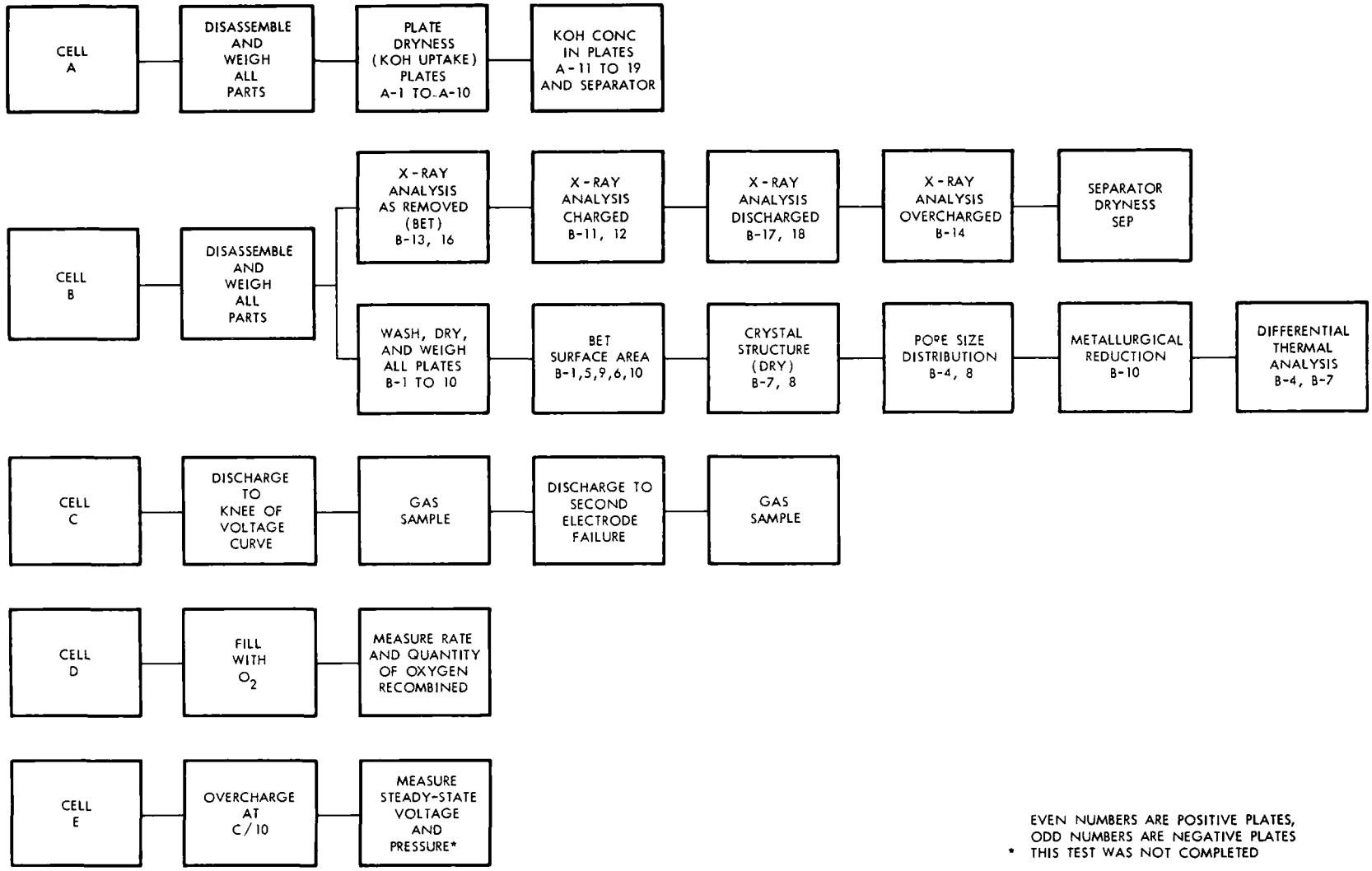

Figure 2. Cell Analysis Test Program

Gulton were weighed in the controlled-atmosphere chamber, and this weight was considered to be the weight in the "as removed" condition. The plates and separators of cells A and B were analyzed as indicated in Figure 2.

Tests performed on cells C, D, and E at Martin Marietta were intended to establish whether the positive or negative was the limiting electrode, the rate of oxygen recombination in the cell, and steady-state pressure and voltage during overcharge. This portion of the test program also is given in Figure 2.

In the remainder of this report, the individual tests are described and the results discussed. Selected parts of this report have been prepared by Martin Marietta, Gulton Industries, and ESB Inc. The correlation between battery test number, Gulton group number, and ESB group number is given in Table 1. The date the battery failed and was sent for analysis, and the results of the cycling tests, also are included in the table. The batteries are listed in order of decreasing cycle life and days of operation in Table 2. In Table 3 the manufacturer's cell number and Martin Marietta test cell numbers are listed for analysis test cells A and B. In the remainder of this report, all numbers will be referenced to the Martin Marietta battery number. The cells from the control battery were those that had been given only three sets of conditioning cycles over a three-year period. The results of the analysis of the components of these cells serve as a basis for comparison for the other cells in the test. These cells contained essentially unused material and therefore were designated the control cells for this part of the test program.

The component materials from Batteries 5 and 6 were not analyzed, because these batteries failed very early in the test program and were given extended electrical testing other than cycling tests in an effort to revitalize them. Their characteristics would therefore not have been indicative of the cycling test operation. The cells from Battery 3 were given 180 cycles, allowed to stand on open circuit almost two years, and then reassembled into a test rack and tested as Battery 12.

Two sets of cells from Battery 8 were examined at different respective times as indicated in Table 1. They are designated 8A and 8B.

The AMF 25° and AMF 10° battery data are included in this report for comparison of deeper depth of discharge operation and lower temperature operation against the operation of the Martin Marietta test batteries. The cells came from the same manufacturing period and were operated in the test program (Contract NAS5-2366) at AMF in Alexandria, Virginia, under the

Table 1

Designation and History

Martin Marietta Battery	Gulton Group	ESB Group	Sent for Analysis				Battery Life to Failure		
			Date	Cycles	Days	Order of Analysis	Cycles	Days	Number of Cells Failed
Control	1	BR	3-4-65	9	8	1			--
0	2	BS	4-20-65	3,065	479	2	3,065	479	5
1	12	BD	1-10-66	3,300	722	12	3,928*	940	1
2	3	BT	5-25-65	2,072	370	3	2,072	370	5
4	9	BA	9-29-65	5,418	551	9	5,418	551	5
7	10	BB	12-27-65	2,300	670	10	2,837	830	5
8A	8	BZ	8-31-65	8,033	740	8	8,500*	810	3
8B	16	BH	2-15-66	9,880	900	16	10,218*	940	3
9	15	BG	2-9-66	4,025	605	15	4,582*	688	2
10	7	BY	8-17-65	3,834	515	7	3,834	515	5
11	5	BW	7-20-65	5,793	480	5	5,793	480	5
12	14	BF	1-26-66	3,700	265	14	4,021*	284	2
13	13	BE	1-17-66	5,350	350	13	5,976*	390	0
14	11	BC	1-4-66	1,905	298	11	2,323*	363	0
AMF 25°	4	BU	6-18-65	5,870	513	4	5,870	513	5
AMF 10°	6	BX	8-3-65	6,613	557	6	6,613	557	5

* This battery had not yet failed.

Table 2

Life Test Results

Battery	Cycles	Battery	Days
8	10,218*	8	940*
AMF 10°	6,613	1	940*
13	5,976*	7	830
AMF 25°	5,870	9	688*
11	5,793	AMF 10°	557
4	5,418	5	557
9	4,582*	4	551
12	4,021*	10	515
1	3,928*	AMF 25°	513
10	3,834	6	513
Pack 13 Crane	3,598	11	480
0	3,065	0	479
7	2,837	13	390*
Pack 17 Crane	2,449	2	370
AMF 40°	2,332	14	363*
14	2,323*	Pack 17 Crane	306
2	2,072	12	284*
5	568	AMF 40°	260
6	320	Pack 13 Crane	225

* Battery had not yet failed

Table 3

Cell Designation

Martin Marietta Battery Number	Cell A Number		Cell B Number	
	Martin Marietta	Gulton	Martin Marietta	Gulton
Control	194	2,925	219	2,900
0	208	2,907	213	2,932
1	218	2,906	227	2,916
2	34	3,118	193	2,894
4	20	3,130	23	2,865
7	211	2,922	224	2,905
8A	205	2,911	57	3,113
8B	197	2,926	225	2,899
9	15	3,129	90	2,855
10	212	2,930	215	2,935
11	38	3,153	203	2,902
12	25	2,829	11	3,145
13	22	3,124	35	3,128
14	201	2,891	196	2,931
AMF 25°	5	2,956	6	2,941
AMF 10°	9	2,594	5	2,957

direction of J. M. Sherfey. As can be seen in Figure 1, these cells were operated at a 58% depth of discharge at 25° C and 10° C.

ANALYSIS OF THE COMPONENTS

The test methods used in the analysis of the component materials of cells A and B are described in this section. The component parts of the cell include the positive plates, negative plates, electrolyte, and separator. Each method is described briefly, and the description is followed by a discussion of the test results. The types of tests are separated into four categories: (a) visual inspection, (b) wet methods, including weight analysis, KOH absorption, and KOH retention, (c) instrumental methods, including X-ray diffraction, surface area analysis, pore size distribution, metallurgical reduction, and differential thermal analysis, and (d) cell unit tests, including overdischarge and rate of oxygen recombination.

Visual Inspection

Cells A and B of each battery were both subjected to a visual inspection before being cut open on the milling machine. The inspection included the following:

1. Cell thickness—top, center, and bottom
2. Cell weight
3. Condition of ceramic seal
4. Condition of pinch tube
5. Condition of negative terminal
6. Condition of welds
7. Existence of leaks around ceramic seal, pinch tube, and welds. (This check was performed by spraying areas to be examined with phenolphthalein indicator.)
8. Peculiarities or special notes

Two general observations were made during the visual inspection. Epoxied terminals were found on each cell, and indentations were found in the walls of the cell cases. During the early stages of the battery test, the tops of the cells were potted to ensure against leaks. Leaks were not found on any of the analysis test cells except the cells from the control battery, which exhibited indications of a leakage. The second observation was of indentations on the side of the cell which were caused by shims installed between the steel plate retainer at the sides of the cell and the cell can itself. These shims had been added because some of the cell walls were concave. The cell walls had been expanding during the charge phase until the can wall met the retainers.

The shims maintained pressure on the can wall even when the wall was in the concave condition. Table 4 includes a compilation of the thickness measured at the top, center, and bottom of the can. Note that the control cells which had no shims were quite prismatic, while those in the cycling test program were affected by the shims to the extent of 30 to 60 mils. The AMF 25° and AMF 10° have somewhat expanded sides.

A visual inspection was made of the pack structure after milling open the can and extracting the cell pack. In all instances, except for the packs from the cells of the control battery and Battery 0, the separators had adhered to the negative plate. Adhesion of the separator to a plate varied from 30% to 100% of the plate area. The most adhesion occurred at the outer plates, the amount tended to diminish toward the center of the pack. The greatest adhesion on the partially adhering plates tended to occur at the center of the plate and may have been partially due to the force exerted by the shims.

Table 4

Cell Thickness

	Cell A			Cell B		
Battery	Top	Center	Bottom	Top	Center	Bottom
Control*	.812	811	.812	.814	.818	.811
0	.803	753	.818	.812	.753	.817
1	.812	753	.819	.809	.759	.819
2	.803	784	.801	.801	.747	.810
4	.806	.750	.801	.809	.785	.818
7	.811	.767	824	.808	.731	.816
8A	.811	.752	819	.805	.738	.800
8B	.810	.780	.822	.811	.751	.821
9	.804	.765	.802	.812	.729	.819
10	.812	754	.816	.810	.766	.812
11	.807	802	.820	.808	.786	.820
12	.820	803	.820	.810	.800	.823
13*	.807	.819	.809	.802	.816	.807
14	.807	.781	811	.810	.790	.816
AMF 25°*	.809	.845	822	.805	.827	.814
AMF 10°*	.814	.863	.822	.809	.833	.823

*No shims.

Other interesting observations appearing in the statements from the Gulton inspection are that both cells from Battery 8A and one cell from Battery 10 had moist separators. Also, the cells from Batteries 4, 7, and 8B contained a black coating on the surface of the ceramic close to the terminal. Blistering of the two positive electrodes was noted in one of the cells from Battery 2.

Statements concerning the visual inspection of the cell components are summarized in Table 5.

Table 5

Inspection Notes on Internal Cells

Battery	
Control	None.
0	None.
1	Both cells—Extreme adhesion of separator to negative plate.
2	Both cells—Dendrites around ceramic of positive terminal. Cell A—Blistering of top and bottom edges of plates A-8 and A-14—heavy adhesion to all negatives beginning with A-1 and diminishing through cell. Most adhesion in center of plate. Cell B—Slight separator adhesion to plate B-19—rest of cell O.K.
4	Both cells—Separator adhesion to 75%-90% of all negative plates. Crystals on positive comb support. Ceramic was black on inside.
7	One cell—Crystals on positive comb support—ceramic black.
8A	Both cells—Separator very moist—60%-100% adhesion of separator to negative plates.
8B	Both cells—Ceramic black—KOH crystals on inside comb support.
9	Both cells—Separator adhesion on plates 1 and 3 at a minimum, increasing to 70%-90% through the cells.
10	Both cells—Separator adhesion to 30%-90% of surface area of all negative plates. One cell—Separator was moist—least adhesion in center of cell.
11	Both cells—Separator adhesion on outside plates—least on inside plates. One cell—Plate adhered to inside case.
12	None.
13	One cell—Extreme adhesion to negative plates.
14	Both cells—Strong separator adhesion.
AMF 25°	Both cells—Separators dry and black—outer negative plates welded to surface of case.
AMF 10°	One cell—100% adhesion of separator to negative plates. Other cell—Intermittent adhesion.

Wet Methods

Weight Analysis--Washing and Drying—Plates 1 through 10 from cell B were removed from the cell container, separated, and weighed in an argon atmosphere. They were then packed individually into plastic bags and sealed in a Mason jar filled with argon. The plates were transferred to the ESB Inc. Research Center for surface studies. Soon after arrival, the jar was opened. The plates were removed and washed free of alkali, dried in a vacuum oven overnight at 45° C, and then cooled in a desiccator. They were then weighed, to determine the weight loss due to washing, after they had reached thermal equilibrium in the laboratory atmosphere. In some instances, the adhering separator could not be removed without physical damage to the plate.

The results of the negative plate weighings are given in Table 6 and Figure 3. The average negative plate weight is for electrodes numbered 3, 5, 7, and 9. Plate 1, the outside plate, also was weighed, but it was not considered in the average.

Table 6

Negative Plate Weights

Battery	Average Weight (gm)		Δ(gm)	Average Δ/gm**	Operation	
	As Received	Washed & Dried			Cycles	Days
Control	8.01	7.02	.99	.14	---	---
0	7.87	6.81	1.06	.16	3,065	479
1	8.19	6.83	1.36	.20	3,928*	940
2	7.88	6.80	1.08	.16	2,072	370
4	7.86	6.70	1.16	.17	5,418	551
7	7.84	6.72	1.12	.17	2,837	830
8A	7.96	6 64	1.32	.21	8,500*	810
8B	8.06	6.85	1.21	.18	10,218*	940
9	7.95	6.86	1.09	.16	4,582*	688
10	7.83	6.69	1.14	.17	3,834	515
11	8.09	6.76	1.33	.20	5,793	480
12	8.12	6 95	1.17	.17	4,021*	284
13	8.47	7.26	1.21	.17	5,976*	390
14	8.09	6 99	1.10	.15	2,323*	363
AMF 25°	7 87	6.42	1.45	.23	5,870	513
AMF 10°	7.85	6.65	1.20	.18	6,613	557
Average	8.00	6.81	1.19	.18		

* Battery had not yet failed.

** Weight gain from KOH absorption, as inferred from weight loss due to washing and drying.

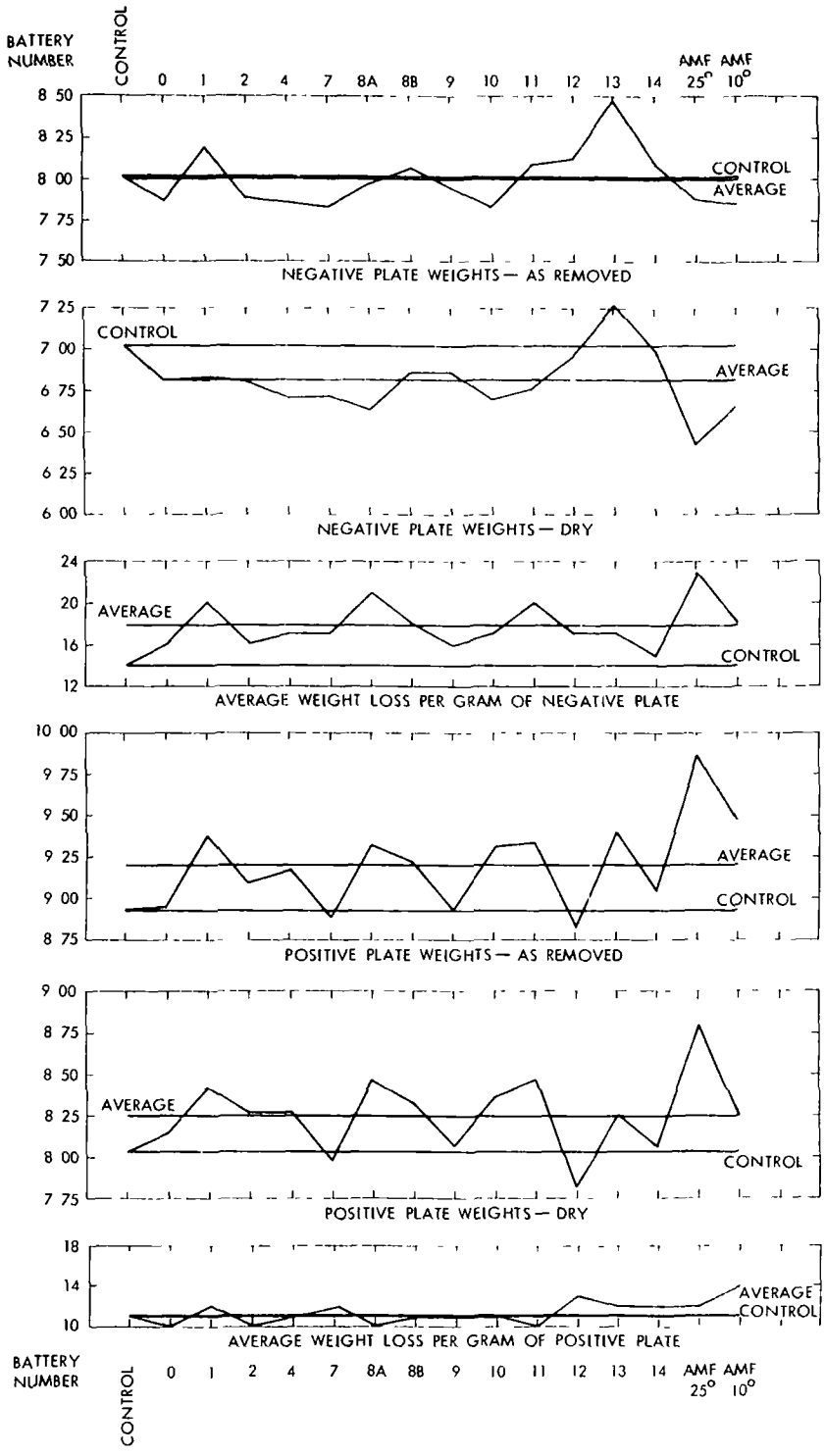

Figure 3. Plate Weights and Loss in Weight Due to Washing and Drying

Note that the weight loss due to washing for the control battery (only three sets of conditioning cycles) was lower than for any of the other batteries. The dry weight is also higher than for the others except Battery 13. The AMF 25° battery had the lowest washed and dried plate weight (see Table 6). The generally higher weight loss for plates from cells which had been operated for prolonged periods was, from all indications, due to the electrolyte that transferred from the separator into the plate during the battery test.

The positive plate weights are summarized in Table 7 and compared in graphic form in Figure 3. Average weight change varied from 10% to 14%,

Table 7

Positive Plate Weights

Battery	Average Weight (gm)		Δ(gm)	Average Δ/gm†	Operation	
	As Received	Washed & Dried			Cycles	Days
Control	8.95	8.04	.91	.11	---	---
0	8.95	8.14	.81	.10	3,065	479
1	9.38	8.42	.96	.12	3,928*	940
2	9.10	8.26	.84	.10	2,072	370
4	9.17	8.26	.91	.11	5,418	551
7	8.88	7.98	.90	.12	2,837	830
8A	9.32	8.46	.86	.10	8,500*	810
8B	9.22	8.32	.90	.11	10,218*	940
9	8.93	8.07	.86	.11	4,582*	688
10	9.31	8.37	.94	.11	3,834	515
11	9.34	8.47	.87	.10	5,793	480
12	8.83	7.81	1.02	.13	4,021*	284
13	9.39	8.25	1.14**	.14	5,976*	390
14	9.01	8.05	.96	.12	2,323*	363
AMF 25°	9.86	8.80	1.06	.12	5,870	513
AMF 10°	9.46	8.26	1.20	.14	6,613	557
Average	9.19	8.25	.94	.11		

* Battery had not yet failed.

** One plate was 1.86.

† Δ = weight gain from KOH absorption, as inferred from weight loss due to washing and drying.

with the control battery averaging 11%. The results are the average of the five plates numbered 2, 4, 6, 8, and 10.

The average weight loss for the negatives is 18%, while the average for the positives is 11%.

KOH Absorption—The uptake, or absorption, of KOH by the plates is an indication of plate dryness—the higher the uptake, the drier the plate. The results of this method of analysis are given in Table 8. The following procedure was used:

1. With a pair of tongs (and, if necessary, a spatula), the plate was lifted off, weighed, and recorded.
2. The plate was immersed in 36° Bé KOH and agitated for two to three minutes to ensure complete saturation of the plate.
3. With the tongs, the plate was removed from the KOH, and excess KOH was allowed to drip off. The plate was then pulled over the edge of a small glass jar in order to scrape off any surplus KOH. Both sides of the plate were so treated. A flat, nonreflective surface rather than a glossy, reflective surface was deemed to indicate that sufficient KOH had been scraped off.
4. The plate was reweighed.
5. The plate was inserted into a sealable plastic bag (labeled A-1) which was set aside with the bag containing the case and cover of cell A.
6. Steps 1 through 5 were repeated for the next nine plates.

Three sections of the separator also were subjected to the KOH absorption test. In most instances (of the 32 cells analyzed), though, the separator adhered so strongly to the surfaces of the plates that it was not possible to obtain a suitable sample.

It is noteworthy that the percentage of increase in weight of the negatives due to the KOH absoprtion is almost twice that of the positives. This agrees with the pattern found in determining weight loss under "Weight Analysis—Washing and Drying," above, where the negatives were wetter and lost almost twice as much as the positives from washing and drying. Clearly, the negatives seem to have almost twice the ability that the positives do to absorb KOH. (In the KOH absorption test, it should be remarked, the amount of KOH absorbed averaged only 1/7 or 1/8 as much as the amount indicated under "Washing and Drying.")

Table 8

KOH Absorption

Battery	Negatives Average Weight		Average % Increase*	Positives Average Weight		Average % Increase*	Separator Average % Increase	Operation	
	As Removed	After Dip		As Removed	After Dip			Cycles	Days
Control	8.13	8.22	.90	8.93	9.02	.96	186	-	-
0	7.97	8.09	1.50	8.91	9.00	.98	188	3,065	479
1	8.11	8.34	2.87	9.15	9.23	.89	196	3,928**	940
2	7.92	8.05	1.63	8.96	9.06	1.08	215	2,072	370
4	7.90	8.04	1.72	9.01	9.11	.82	-	5,418	551
7	7.92	8.07	1.81	9.06	9.17	1.17	126.5	2,837	830
8A	8.02	8.16	1.73	9.21	9.25	.43	-	8,500**	810
8B	8.15	8.25	1.25	9.07	9.16	1.22	205	10,218**	940
9	8.07	8.18	1.46	8.93	9.02	.96	178	4,582**	688
10	7.95	8.05	1.23	9.31	9.38	.67	-	3,834	515
11	8.04	8.12	.99	9.34	9.48	.89	-	5,793	480
12	7.88	7.99	1.36	9.21	9.29	.91	237	4,021**	284
13	8.26	8.50	2.91	9.81	9.92	1.08	272	5,976**	390
14	8.00	8.16	2.00	9.42	9.51	.93	145	2,323**	363
AMF 25°	7.83	7.98	1.93	9.46	9.59	1.32	-	5,870	513
AMF 10°	8.01	8.14	1.71	9.61	9.71	.98	186.5	6,613	557
Average	8.01	8.15	1.68	9.18	9.31	.96			

* Based upon increases of individual plates.
** Battery had not yet failed.

Battery 10 and 11 negative electrodes absorbed the least KOH and therefore were markedly wetter than most of the other battery plates. Examination of positive plate data reveals a wide variation in percentage of increase, from 0.43 for Battery 8A to 1.32 for AMF 25°.

KOH Retention—The purpose of this test was to determine how much $(OH)^-$ was available in each of the plates after the degradation processes caused by the cycling had taken place. The following procedure was used:

1. With a pair of tongs and a spatula, the plate was lifted off and weighed.
2. The plate was immersed in a beaker (labeled A-11 for plate A-11) of deionized water and agitated several moments with the tongs.
3. Steps 1 and 2 were repeated on the ensuing plates and Separator A, modifying Step 2 so that the beakers were labeled A-12, A-13. . . A-19 and Separator A.
4. Each plate and the separator were agitated about once every half hour.
5. The plates and separator were allowed to stand overnight in individual sealed beakers. The following morning each plate was lifted out of its beaker with the tongs and, with the plate being held over the beaker from which it had been taken, the plate was rinsed with fresh deionized water from a plastic squeeze bottle. All drippings fell into the beaker. The surplus liquid was wiped off the surface of the plate by pulling the plate over the edge of its beaker. Surplus liquid was removed from the separator by squeezing it.
6. Each plate and the separator were then placed into individual sealable plastic bags, each bag being labeled the same as the beaker from which the plate (or separator) was taken, and being added to the remainder of the bags set aside from cell A.
7. Each beaker of extract was titrated to determine the KOH content.

It would be difficult to establish a specific trend from the data given in Table 9. The control battery positive and negative plates are lower in $(OH)^-$ concentration than are the plates for most of the other batteries. The Battery 0 titration results appear to be low for positive, negative, and separator. In all instances except Batteries 2, 10, and AMF 10° there appears to be more available $(OH)^-$ in the negative plate than in the positive, even though (as will be seen in a later section) there is 20 times more surface area in the positives than in the negatives.

Gulton Analysis of Wet Test Methods—Gulton Industries, in addition to performing tests on the components of the cell, performed a statistical evaluation of the weight analysis, KOH retention, and KOH absorption data. This

Table 9

KOH Titration—mg/gm of KOH in Plates
(Average of 4 plates)

Battery	Negatives	Positives	Separator
Control	24.51	20.95	88.5
0	19.52	17.97	118.6
1	32.65	27.73	134.0
2	26.25	28.32	127.5
4	30.72	25.85	123.1
7	25.83	23.93	130.2
8A	30.18	26.54	120.9
8B	32.32	31.17	154.3
9	27.75	26.27	118.6
10	23.48	27.10	121.0
11	37.08	31.45	97.8
12	33.38	30.36	140.9
13	35.33	30.79	118.2
14	32.19	28.31	140.7
AMF 25°	35.05	33.92	62.7
AMF 10°	27.24	36.34	45.0
Average	29.59	27.93	115.1

work appears in their final report to Martin Marietta (Reference 4). Its findings are, in part, as follows. As a final analysis, the comparison of plate weights from cells of the various batteries in the test program has been examined to determine if significant battery differences are present. The Analysis of Variance technique was used in this comparison. A table was prepared* with two variables of classification, in which the means, sum of squares, and mean squares were determined and the F ratio was formed to test for significant differences. Gulton reported that the tests showed significant differences with better than .999 confidence existing between the control battery, Battery 13, and AMF 25°. The data from the control battery were significantly below, and the data from Battery 13 and AMF 25° were significantly above, the average for all batteries tested. These three batteries were significantly non-random with .99 confidence.

*See Figure 4 in this document (corresponding to Figure 7 of Reference 4).

PAGE MISSING FROM AVAILABLE VERSION

BATTERY NUMBER	TOTAL PLATE WEIGHT	POSITIVE PLATE WEIGHT	NEGATIVE PLATE WEIGHT	SEPARATOR WEIGHT	TOTAL PLATE Mg KOH	POSITIVE PLATE Mg KOH	NEGATIVE PLATE Mg KOH	SEPARATOR Mg KOH	TOTAL PLATE DRIED WEIGHT	POSITIVE PLATE DRIED WEIGHT	NEGATIVE PLATE DRIED WEIGHT	TOTAL PLATE WEIGHT DIFFERENCE	POSITIVE PLATE WEIGHT DIFFERENCE	NEGATIVE PLATE WEIGHT DIFFERENCE	TOTAL PLATE ELECTROLYTE ABSORPTION	POSITIVE PLATE ELECTROLYTE ABSORPTION	NEGATIVE PLATE ELECTROLYTE ABSORPTION	Σ_i	$\bar{x}$
Control	0	-1	1	0	-3	-3	-3	-1	0	-2	1	-2	-1	-3	-2	0	-2	-21	-1 24
0	-1	-1	0	1	-3	-3	-3	1	-1	-1	0	-1	0	-3	-1	0	-1	-17	-1 0
1	1	0	1	-1	1	0	1	0	1	1	0	2	0	3	3	0	3	+16	941
2	-1	-1	0	1	-1	0	-1	1	0	0	0	-2	-3	-3	0	0	0	-10	- 589
12	-1	-1	0	0	2	0	2	1	-1	-3	1	1	2	-3	-1	0	-1	-2	- 118
4	-1	-1	-1	0	-1	-1	0	0	-1	0	-1	0	-1	0	0	0	0	-8	- 470
13	3	1	3	-1	3	0	3	-1	1	0	3	1	0	1	3	1	3	+24	1 41
14	0	0	1	0	-1	0	-1	1	0	-1	1	-1	0	-2	1	0	1	-1	- 059
7	2	-1	-1	1	-3	-1	-2	1	-1	-3	-1	-1	-1	-1	1	1	0	-10	- 589
8	0	-1	0	0	-1	-1	0	0	0	2	-1	1	-3	3	-1	-2	0	-4	- 235
8A	0	-1	1	-1	1	1	1	1	1	1	0	0	-1	1	-1	0	-1	+3	176
9	-1	-1	0	1	1	-1	-1	1	-1	-1	0	-1	-2	-2	-1	0	-1	-12	- 706
10	0	1	-1	0	1	-1	1	1	0	1	-1	-1	0	-1	-2	-1	-2	-5	- 294
11	0	1	0	-1	3	2	3	-1	1	2	0	1	-2	3	-3	-1	-3	+5	294
AMF 25°	3	3	0	-1	3	3	3	-2	1	3	-3	1	3	1	2	2	1	+23	1 35
AMF 10°	2	3	0	-1	3	3	-1	-3	-1	1	-1	3	3	1	1	0	1	+14	824
Σ_i	+6	0	+4	-2	+3	-2	+2	0	-1	0	-2	+1	-6	-5	-1	0	-2	-5	
$\bar{x}$	375	0	25	- 125	188	- 125	125	0	- 062	0	- 125	062	- 375	- 312	- 062	0	- 125		- 0183

Note This summary is derived from Figure 7 of Reference 4, accordingly, the weights upon which it is based will not necessarily agree with those in Tables 6, 7, and 8

0 = A = Average
+1 = AA = Above Average
+2 = SAA = Significantly Above Average (95%)
+3 = SAA = Significantly Above Average (99%)
-1 = BA = Below Average
-2 = SBA = Significantly Below Average (95%)
-3 = SBA = Significantly Below Average (99%)

Figure 4. Summary of Analysis of Means for Analysis of Variance (rankings represented numerically)

PAGE MISSING FROM AVAILABLE VERSION

Instrumental Analysis

X-Ray Analysis—The two purposes of performing the X-ray diffraction analysis were: (a) to determine what constituent crystalline materials were present and whether impurities appeared as crystalline compounds after cycling for extended periods of time, and (b) to determine whether the effects of charge and discharge are related to crystalline changes in the materials of the plates.

X-ray diffraction analysis was performed on plates both in the as-removed condition in sealed polyethylene bags and in the washed and dried condition. The purpose of making a measurement in the sealed bag was to avoid reaction of the damp electrode plates with the CO_2 from the air. The procedure resulted, however, in a high background on each diffraction measurement. Both the wet and dry plate analyses were performed using a Norelco X-ray diffraction instrument.

The wet-plate diffraction analysis included electrodes B-11 through B-18 from cell B. Plates B-13 (negative) and B-16 (positive) were analyzed in the as-removed condition. The samples used in the analysis were cut from each plate as shown in Figure 5.

Plates B-11 and B-12 were placed into a test cell filled with 36° Bé KOH. The test cell was subjected to a charge in a manner similar to that utilized in the battery cycling program and at the same current density for the specific battery of which the cell was a part. Upon completion of the charge, the cell was returned to a glove box and dismantled and the plates were cut, sealed in a bag, and submitted to X-ray analysis. Plate B-14 was installed in a laboratory cell and given an extended overcharge at C/10 for 16 hours. It was also sealed in a polyethylene bag and given an X-ray diffraction analysis. Plates B-17 and B-18 were discharged in the same manner as the battery from which they were removed in the test program. The discharge was continued until failure of each plate. The plates were then sealed in a bag and given an X-ray analysis. Thus the analysis of the seven plates gave information on the crystal structure and impurities in

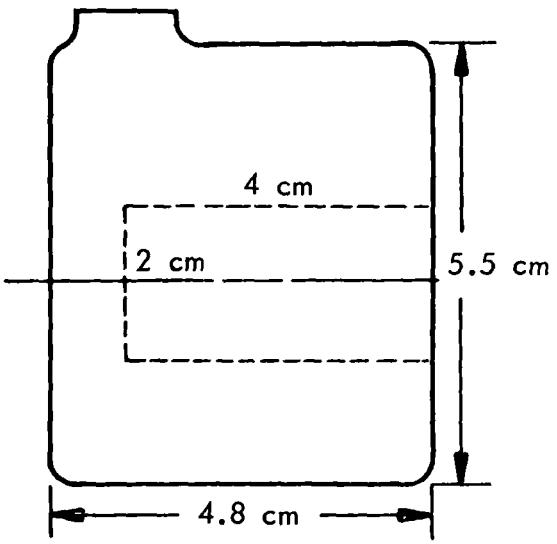

Figure 5. Cutout for X-Ray Analysis (cuts were made on dotted lines; dimensions approximate)

the discharged, the as-is, and the charged condition for positive and negative plates, and similar information for the overcharged condition for a positive plate.

Negative plate B-7 and positive plate B-8 were among those plates sent in the dry condition to the ESB Inc. Research Center for analysis. Both were subjected to an X-ray analysis using a Norelco X-ray diffraction unit. The dry plates were not packaged in polyethylene; but were inserted into the sample holder in the dry condition, and a scan was made across the surface. In addition, some of the plates after being surface-analyzed were ground up and an X-ray diffraction analysis was performed on the bulk material.

The X-ray data for the dry negative and positive plates are found in Table 10. Much of the identification of the dry-plate materials has been made by ESB in its final report (Reference 5). The ESB tables were modified and put into the format shown, which is more directly related to the battery test program.

Negative Plates—For the negative plates, there is some variation in diffraction peaks because of the variation in surface when the sample was mounted in its holder for analysis. However, as expected, cadmium hydroxide (Cd $(OH)_2$) and nickel (Ni) from the sintered matrix were the major constituents of all negative plates analyzed. Cadmium metal was found as a minor constituent on the surface of all plates analyzed except in the control battery and Battery 2. However, when the Battery 2 material was analyzed as bulk material, it also proved to contain cadmium metal. Surprisingly, the two additional compounds identified as minor constituents of the negative plates were cadmium carbonate ($CdCO_3$) and gamma cadmium hydroxide (γCd $(OH)_2$). A comparison between Battery 2 surface and bulk diffraction patterns indicates that the $\gamma Cd(OH)_2$ may be found inside the negative plates. It appeared also on the surface only when subjected to greater operating stresses such as those of the AMF 25° test cells.

The second objective of performing the X-ray diffraction analysis, namely, to determine the effects of charge and discharge on the plate materials, was more difficult to achieve. First, it was difficult because the technique of performing X-ray analysis on plates in the wet condition sealed within polyethylene bags was used. This technique resulted in high background and masking of peaks because of the polyethylene. Second, there was a significant difference between plates in the same cell container. The intensities and X-ray analysis of the wet plates are listed

Table 10

Results of X-Ray Diffraction Analysis of Dry Plates

Battery	Negative Plate		Positive Plate	
	Major	Minor	Major	Minor
0	Ni, $Cd(OH)_2$		Ni, $Ni(OH)_2$	
1	Ni, $Cd(OH)_2$	Cd	Ni, $Ni(OH)_2$, $CaCO_3$	
2	Ni, $Cd(OH)_2$	Cd	Ni, $Ni(OH)_2$	
2 (bulk)	Ni, $Cd(OH)_2$	Cd, $\gamma Cd(OH)_2$	Ni, $Ni(OH)_2$	
4 (bulk)			Ni, $Ni(OH)_2$	
4	Ni, $Cd(OH)_2$	Cd, $CdCO_3$	Ni, $Ni(OH)_2$, $CaCO_3$	β NiOOH
12	Ni, $Cd(OH)_2$	Cd, $CdCO_3$	Ni, $Ni(OH)_2$, $CaCO_3$	β NiOOH, $Cd(OH)_2$
13	Ni, $Cd(OH)_2$	Cd, $CdCO_3$	Ni, $Ni(OH)_2$, $CaCO_3$	
14	Ni, $Cd(OH)_2$	Cd, $CdCO_3$	Ni, $Ni(OH)_2$, $CaCO_3$	
7	Ni, $Cd(OH)_2$	Cd, $CdCO_3$	Ni, $Ni(OH)_2$, $CaCO_3$	β NiOOH
8A	Ni, $Cd(OH)_2$	Cd, $CdCO_3$	Ni, $Ni(OH)_2$	β NiOOH, $CaCO_3$
8B	Ni, $Cd(OH)_2$	Cd, $CdCO_3$	Ni, $Ni(OH)_2$, $CaCO_3$	
9	Ni, $Cd(OH)_2$	Cd, $CdCO_3$	Ni, $Ni(OH)_2$, $CaCO_3$	
10	Ni, $Cd(OH)_2$	Cd, $CdCO_3$	Ni, $Ni(OH)_2$	$Cd(OH)_2$, $CaCO_3$
11	Ni, $Cd(OH)_2$	Cd, $CdCO_3$	Ni, $Ni(OH)_2$, $CaCO_3$	
AMF 25°	Ni, $Cd(OH)_2$	Cd, $CdCO_3$, $\gamma Cd(OH)_2$	Ni, $Ni(OH)_2$, $CaCO_3$	
AMF 10°	Ni, $Cd(OH)_2$	Cd	Ni, $Ni(OH)_2$, $CaCO_3$	$Cd(OH)_2$

in Table 11. The ratios of peak heights ($Cd(OH)_2$/Cd/Ni, where Ni was set equal to 10.0) are compared in the table. It is difficult to abstract a particular characteristic from these data.

Table 11

Ratio of Intensities of Negative Plate Materials

$Cd(OH)_2$/Cd/Ni = x/y/10

(100) (100) (42)

Battery	Discharged	As Removed	Charged
Unoperated plate	-	5.8/2.6/10.0	
Control	-	6.6/1.8/10.0	2.3/4.6/10.0
0	-	5.0/2.3/10.0	1.9/3.8/10.0
1	1.7/1.0*	1.9/1.0*	1.6/1.0*
2	-	3.0/ 1.3/10.0	1.7/6.7/10.0
4	13.3/6.0/10.0	313.0/40.0/10.0	12.1/6.4/10.0
12	12.1/2.2/10.0	11.3/4.5/10.0	8.3/3.8/10.0
13	8.2/3.5/10.0	33.5/7.1/10.0	2.6/2.3/10.0
14	14.6/1.9/10.0	49.0/18.2/10.0	17.0/7.4/10.0
7	14.5/2.8/10.0	1.8/10.3/10.0	4.6/0.9/10.0
8A	5.7/2.9/10.0	14.1/5.9/10.0	41.7/22.0/10.0
8B	22.0/14.0/10.0	7.9/3.7/10.0	26.7/23.4/10.0
9	22.0/7.8/10.0	15.9/4.1/10.0	8.3/3.3/10.0
10	20/10/10	4.3/2.2/10.0	0.4/13.6/10.0
11	3.1/1.0*	125/40/10	10.6/15.6/10.0
AMF 25°	103/33.3/10	35.0/8.6/10.0	10.9/15.9/10.0
AMF 10°	20/4.3/10	39 4/2 6/10 0	7.7/2.0/10.0

* Ni peak not given.

Positive Plates—The positive plates in the wet and dry condition also were analyzed using the X-ray diffraction method. Listed in Table 10 are the peaks for the constituents of the dry plates. In all cases the major peaks were due to the nickel of the sintered matrix and nickel hydroxide of the active material. It is interesting to note the unusual appearance of calcium carbonate as a major constituent of the positive plate surface in 11 samples.

By performing the analysis on the surface material and the bulk material as was done for Battery 4, it was shown that the $CaCO_3$ was a surface

constituent and did not appear in the bulk. This finding differed from that for the gamma cadmium hydroxide in the negative material, which appeared in bulk but not on the surface. The ESB report suggested that the calcium carbonate on the plate surface may have masked the other materials on the surface. The obvious question is: To what extent does the calcium carbonate degrade the positive-plate activity and affect plate life, also where does the calcium come from and where does the carbonate come from? The calcium may have arrived in the cell via the electrolyte or in the water with which the electrolyte is diluted to 30° Bé. The carbonate may come from the oxidation of the separator, which over the cycling life became dry and somewhat warm and came into contact with oxygen gas. It is also interesting to note that cadmium hydroxide was found as a minor constituent in plates of Battery 12, Battery 10, and AMF 10°. The active charged material of the positive βNiOOH was only found in faint traces in Battery 4, Battery 12, Battery 7, and Battery 8A.

The appearance of $CaCO_3$ and $Cd(OH)_2$ on the surface of the positives is also confirmed in some of the X-rays of diffraction patterns of samples run in the wet condition sealed inside the polyethylene bag. The bag was found to mask many of the peaks; nevertheless, it proved possible to make positive identification of the materials in all of these cases, as shown in Table 12.

Surface Area Measurement (BET)—The size of each plate was 4.8 by 5.5 cm, equivalent to an apparent surface area of 52.8 square centimeters for both sides in total. The entire plate was utilized for each BET measurement. The negative plate analyses were prepared on the first, third, and fifth negatives in the cell stack (plates B-1, B-5, and B-9), and the positive plate analyses from the third and fifth positives in the same stack (plates B-6 and B-10).

Each dry plate was sealed into its individual special sample tube of a type developed by Dr. A. J. Salkind, H. J. Canning, and M. L. Block (Reference 6). These tubes were then put onto the manifold system of BET and degassed for three hours at 46-50° C. The degassing temperature was kept below 50° C to avoid loss of active material. Following degassing, the dead space of each sample was measured at liquid nitrogen temperature, using helium gas. After removing any remaining helium gas by again degassing for about an hour at room temperature, the samples were ready for the measurement of surface area.

This was done using nitrogen gas adsorption at liquid nitrogen temperature (References 7 and 8). A sample of the data sheets and the calculations used to get the surface area appears in Reference 5.

Reference 9 describes the basis for using the gas adsorption method and a Fortran IV computer program for calculation of the results.

Table 12

X-Ray Diffraction Analysis of Positive Plates Identified from Gulton Analysis

Battery	Order of Analysis	Discharged B-18	As Removed B-16	Charged B-12	Overcharged B-14
Control	1	C, D	C, D	D	D
0	2	C, D	A, C, D	E, C, D	C, D
1	12	C, D	C, D, F	D, E	D, F
2	3	D	D	D	D
4	9	C, D	C, D, F	D	D
12	14	C, D	C, D, A	C, D	D
13	13	C, D	C, D	C, D, F	D
14	11	C, D	C, D	C, D	D
7	10	C, D, A	C, D	C, D, A	D
8A	8	C, D	A, C, D	A, C, D, F	A, C, D
8B	16	C, D	C, D, F	C, D	C, D
9	15	C, D, A	C, D	C, D	A, C, D
10	7	C, D	C, D	C, D	C, D, F
11	5	C, D	C, D, F	C, D	C, D
AMF 25°	4	C, D	C, D	C, D	C, D
AMF 10°	6	A, C, D, F	A, C, D	C, D	D
Formed Positive Plate			C, D		

Key: A - $Cd(OH)_2$
C - $Ni(OH)_2$
D - Ni
E - Cd
F - $CaCO_3$

The calculations for surface area were derived from Reference 7. The final calculations are taken from a graph on which is plotted

$$\frac{P_2}{P_s} \quad \text{vs} \quad \frac{P_2}{V(P_s - P_2)} \quad ,$$

where V is the volume of gas adsorbed at equilibrium pressure P_2, and P_s is the saturation pressure of the gas. The volume of gas adsorbed when the entire surface is covered by a nonmolecular layer (V_a) is

$$V_a = \frac{1}{\text{slope} + \text{intercept}}$$

and the surface area (Sw) is

$$Sw = \frac{4.25}{\text{slope} + \text{intercept}}$$

when nitrogen gas is used.

The results are given in Table 13. The surface areas of almost all the samples fall into a range of 4 to 10 square meters per plate for the negatives, and 150 to 190 square meters per plate for the positives. The notable cases falling outside these ranges are as follows: higher surface areas—negative plates of AMF 10°, Battery 10, and Battery 4, positive plates of Battery 11, Battery 9, and Battery 8B.

The relatively higher surface area of negative plate B-1 of Battery 1, which was undoubtedly due to the overheating of that plate during degassing, suggests that controlled heating might be a desirable treatment for negative plates if the electrochemical nature of the plate is not unfavorably changed.

Plate B-5 from Battery 1 and plate B-5 from Battery 8A both have a surface area of less than 3 square meters per plate. This value is the lower detection limit for the BET technique employed in these tests.

Taking an average of the surface areas of the positives to be 17 m^2, the widest variation in surface area is about 30%. The negatives, however, exhibit a variation of up to 200%, assuming an average of 8.28 m^2.

Although the negatives exhibit a wide percentage variation from battery to battery, the variation within a single battery from plate to plate is considerably smaller.

Table 13

Surface Area—by Gas Adsorption (BET)

(square meters per plate)

Battery	Analysis Group	Negatives			Positives	
		B-1	B-5	B-9	B-6	B-10
Control	1	6.67	8.65	8.65	190	191
0	2	9.52	8.05	6.72	167	159
1	12	23*	<3	6.66	156	182
2	3	4.12	3.64	6.13	159	164
4	9	15.62	24.07	7.62	156	212
12	14	7.09	9.74	8.70	176	160
13	13	8.18	8.81	7.02	189	190
14	11	3.83	6.81	5.27	190	176
7	10	7.19	12.81	7.23	225	175
8A	8	4.89	<3	7.14	176	155
8B	16	5.93	3.30	6.82	148	147
9	15	9.82	5.74	9.70	158	147
10	7	10.51	6.67	9.28	173	172
11	5	8.39	4.58	8.04	145	148
AMF 25°	4	7.45	9.02	9.49	163	153
AMF 10°	6	16.41	17.22	14.10	170	160
Average		8.28			170	

Each plate had an apparent surface area of 52.8 cm^2.

* Not included in average (was due to overheating).

Pore Size Distribution—The pore size distribution was determined using an Aminco mercury penetrometer. The samples were discs cut from the positive plates as shown in Figure 6. Negative plates were not utilized, because of the error which would result from cadmium amalgamation by the mercury. The discs were cut to a suitable diameter to fit into the penetrometer tube, using a slow-speed, hollow, diamond-impregnated drill.

Total porosity or total pore volume is a measure of the total void space or volume available to the mercury in the porosimeter or to electrolyte in a cell per gram of sample. It becomes more meaningful when related to the distribution graph and maximum and minimum effective pore diameters.

The maximum and minimum effective pore diameters define the range in which 80% of the pores lie. When the maximum effective pore diameter is large, i.e., above 10μ, the pores are distributed over a wide range of sizes. If it is below 10μ or the curve rises rapidly at some applied pressure, a narrow (more uniform) distribution of the pores is indicated. Most of the samples indicate the wide type of distribution. The total porosity and maximum and minimum effective pore diameters are given in Table 14.

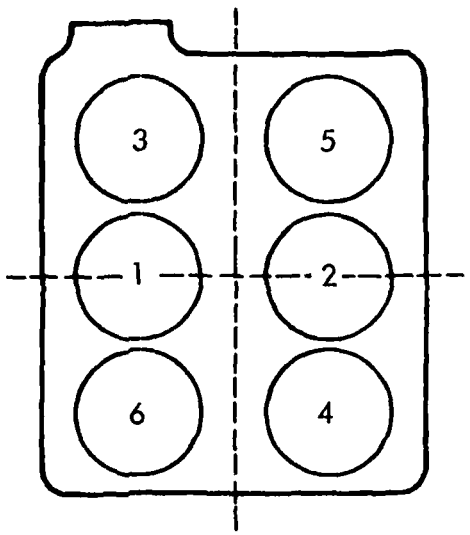

Figure 6. Sample Discs

The reported total porosity and maximum and minimum effective pore diameters both have instrumental limitations. When the 5,000-psi Aminco instrument is used, the pore size range has an upper limit of 100μ and a lower limit of 0.05μ. Higher-pressure instruments (range from 10,000 to 50,000 psi) would extend the minimum effective pore diameter to about 0.004μ and would possibly affect the data on total porosity by detecting smaller pores. The instrument used for these tests does cover most of the pores or volume available to electrolyte.

The total porosity varies from .028 cc/gm to .069 cc/gm (see Table 14). The upper range was achieved on the material from the control battery, which was given three long activation cycles before being sent for analysis. The lowest total porosity is from Batteries 8A and 8B, which were cycled under constant-potential charge operation.

The maximum effective pore diameter (only 10% of the pores were above it) ranged from 3.9 microns to 60.8 microns, while the minimum was lower in most cases than the instrument capability (<.05 microns).

In order to determine the pore size distribution, the volume of mercury required to fill the pores between two limits is plotted vs the limits, Figure 7, in which the pore size distribution D(d) is given as

$$D(d) = \frac{p}{d} \frac{dV}{d(\log d)} \quad ,$$

Table 14

Pore Size Distribution

Battery	Total Porosity (cc/gm)		Maximum Effective Pore Diam (microns)		Minimum Effective Pore Diam (microns)		Plate B-4 D(d)				Plate B-8 D(d)			
							Most Frequent		2nd Most Frequent		Most Frequent		2nd Most Frequent	
							Pore Size (microns)	D(d) Units	Pore Size (microns)	D(d) Units	Pore Size (microns)	D(d) Units	Pore Size (microns)	D(d) Units
	B-4	B-8	B-4	B-8	B-4	B-8								
Control	069	047	60 8	27 2	051	054	75	76	75	60	75	30	3 5	18
0	047	048	3 9	5 9	< 050	050	075	70	3 5	35	3 5	75	075	60
1	050	049	34	40	048	0475	075	66	3 5	35	075	64	7 5	33
2	046	047	5 9	6 5	< 050	054	075	54	1 5	46	075	43	75	33
4	048	052	37	12	053	050	3 5	76	075	73	075	60	7 5	40
12	051	045	39	26	045	049	075	60	1 5	33	075	37	3 5	33
13	056	053	30	55	050	050	075	70	7 5	47	075	60	3 5	50
14	036	056	40	40	045	045	075	70	1 5	33	075	50	7 5	22
7	054	057	28	29 5	040	045	075	73	1 5	40	075	67	1 5	30
8A	033	029	40	38	060	< 05	075	50	3 5	30	075	37	3 5	35
8B	049	031	42	70	049	048	075	50	3 5	45	075	34	1 5	27
9	035	048	43	22	048	048	075	64	1 5	30	075	40	3 5	30
10	041	044	39	60	< 05	< 05	075	70	{15 75	23 23	{075 3 5	50 30	-	-
11	028	045	27	28	< 05	< 05	075	46	3 5	25	075	27	3 5	25
AMF 25°	048	038	30	3 2	< 05	< 05	075	60	75	20	075	87	{75 1 5	13 13
AMF 10°	040	051	30	18	< 05	< 05	3 5	58	075	53	075	43	75	37
Average	046 cc/gm		3 16μ		~ 049μ									

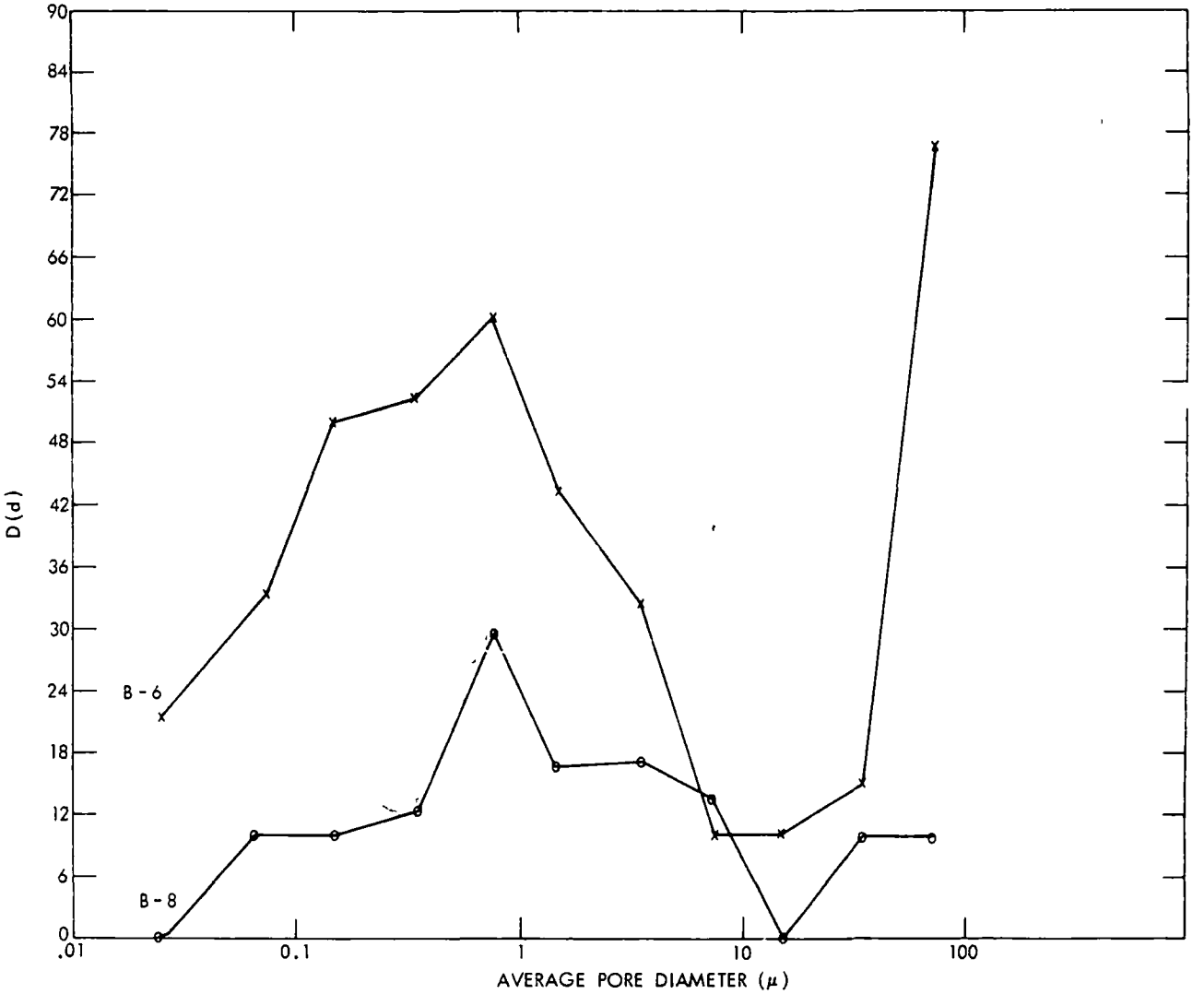

NOTE B-6 RESULTS ARE SHOWN UNDER "B-4" IN TABLE 14

Figure 7a. Pore Size Distribution— Control Battery

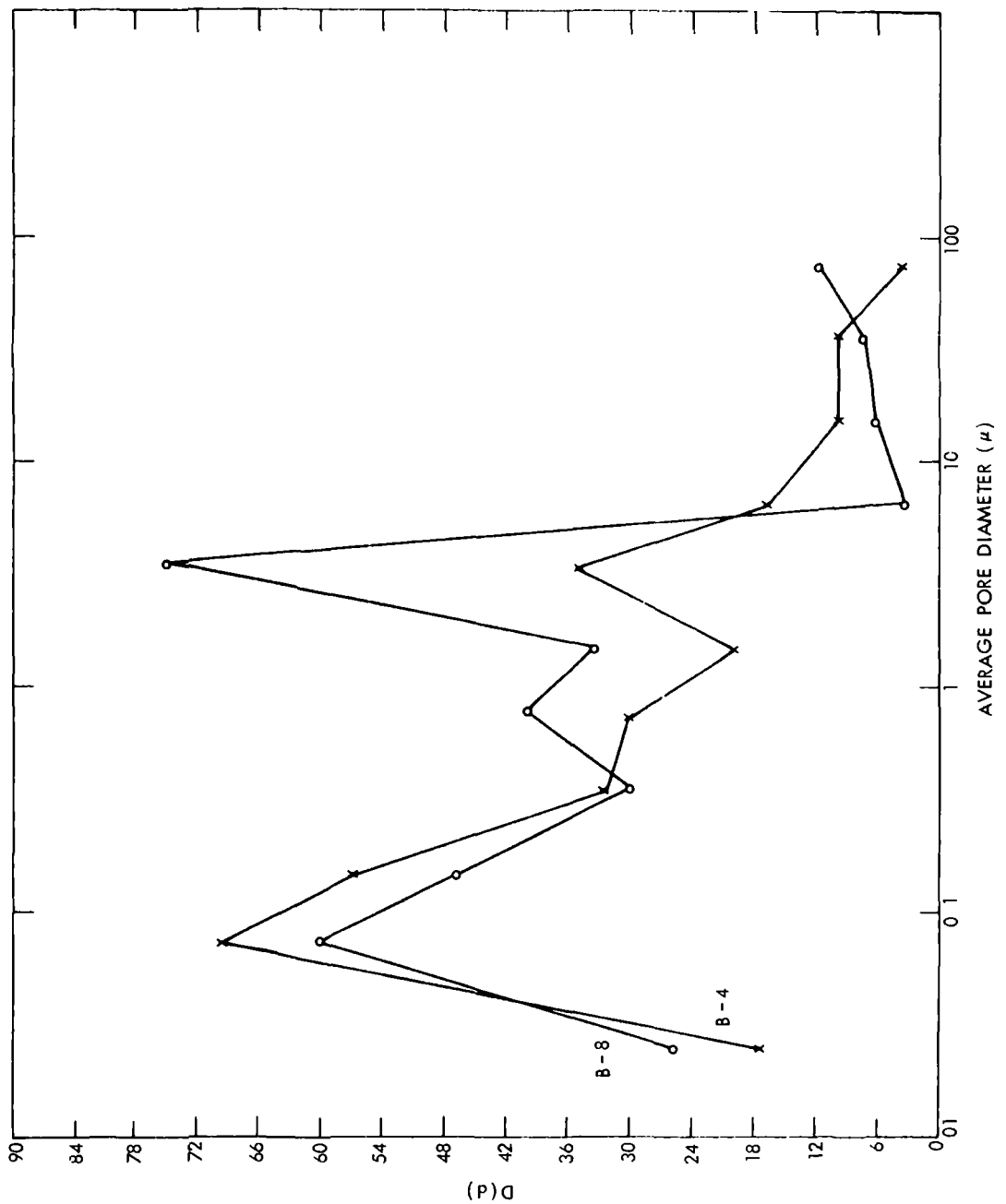
D(d)
90
84
78
72
66
60
54
48
42
36
30
24
18
12
6
0
01
0 1
1
10
100
AVERAGE PORE DIAMETER (μ)
B-8
B-4

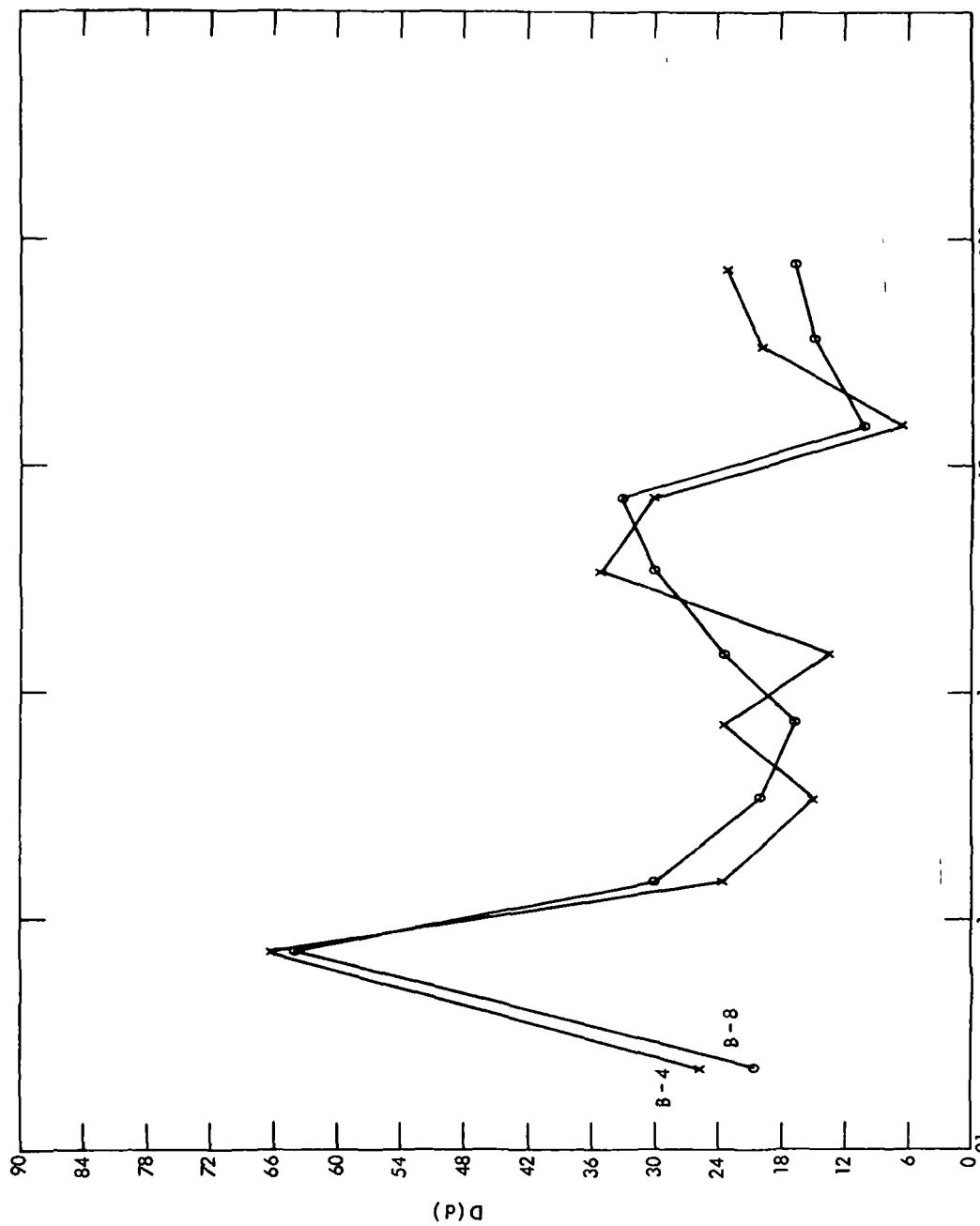

Figure 7c. Pore Size Distribution— Battery 1

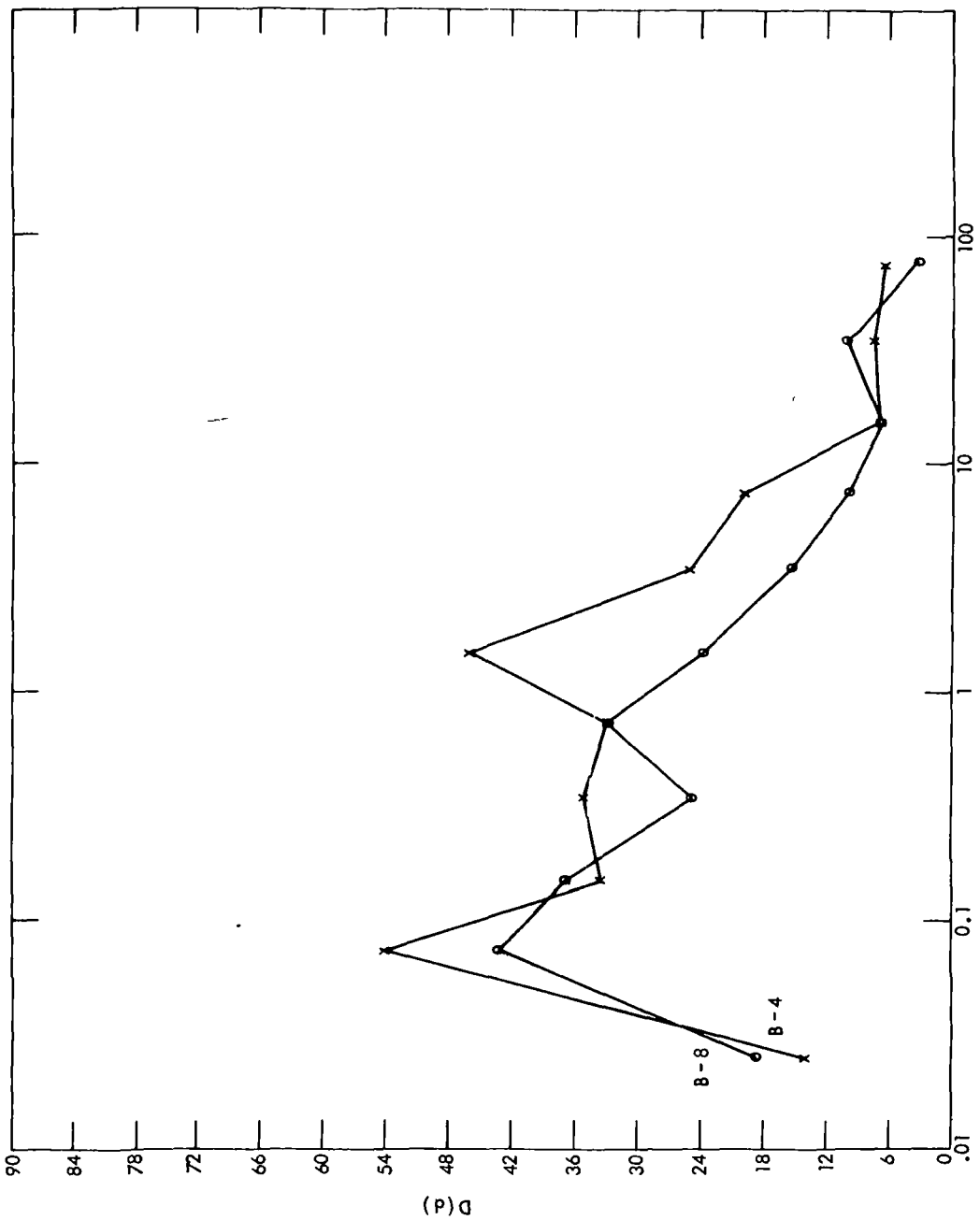

Figure 7d. Pore Size Distribution— Battery 2

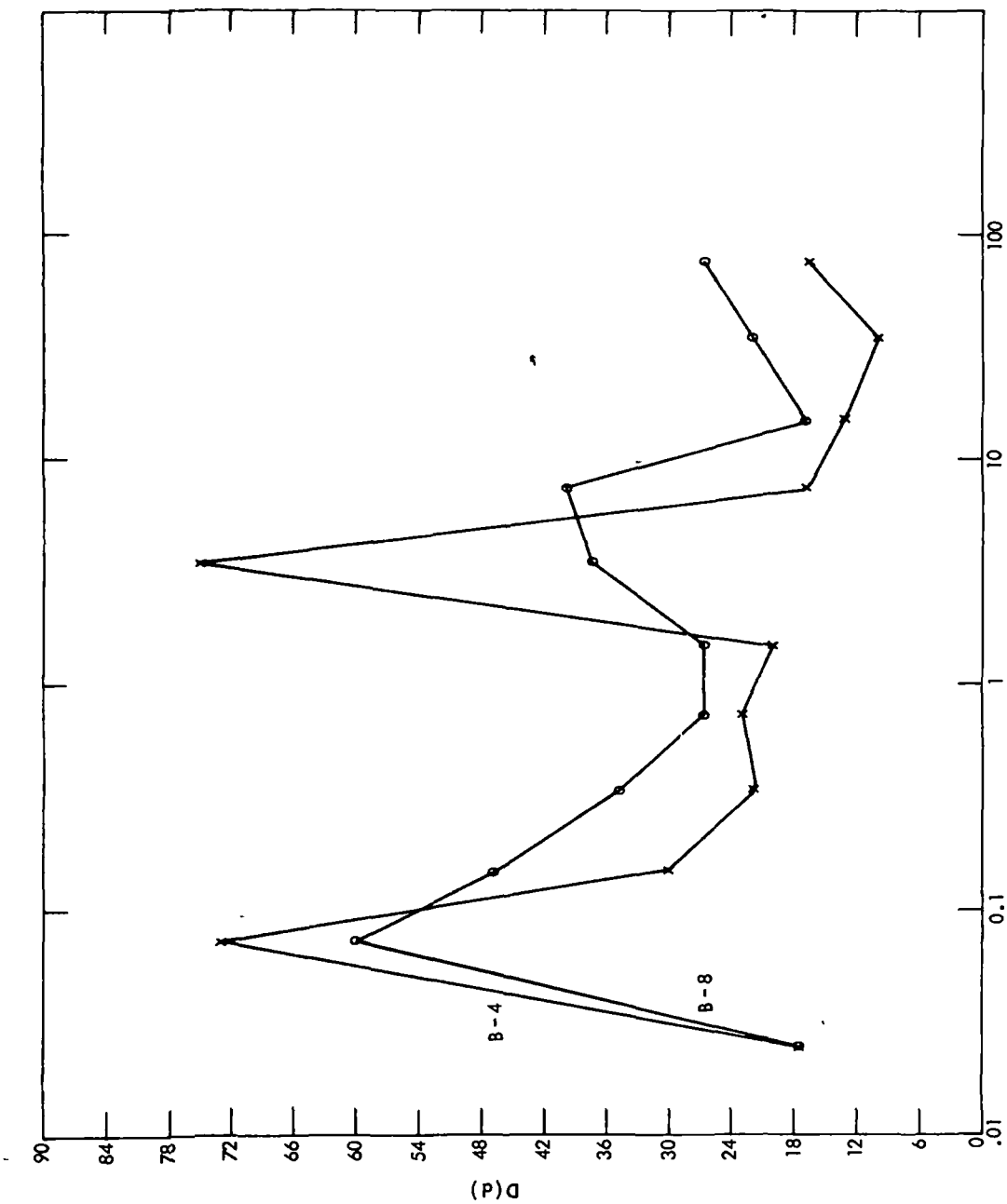

Figure 7e. Pore Size Distribution— Battery 4

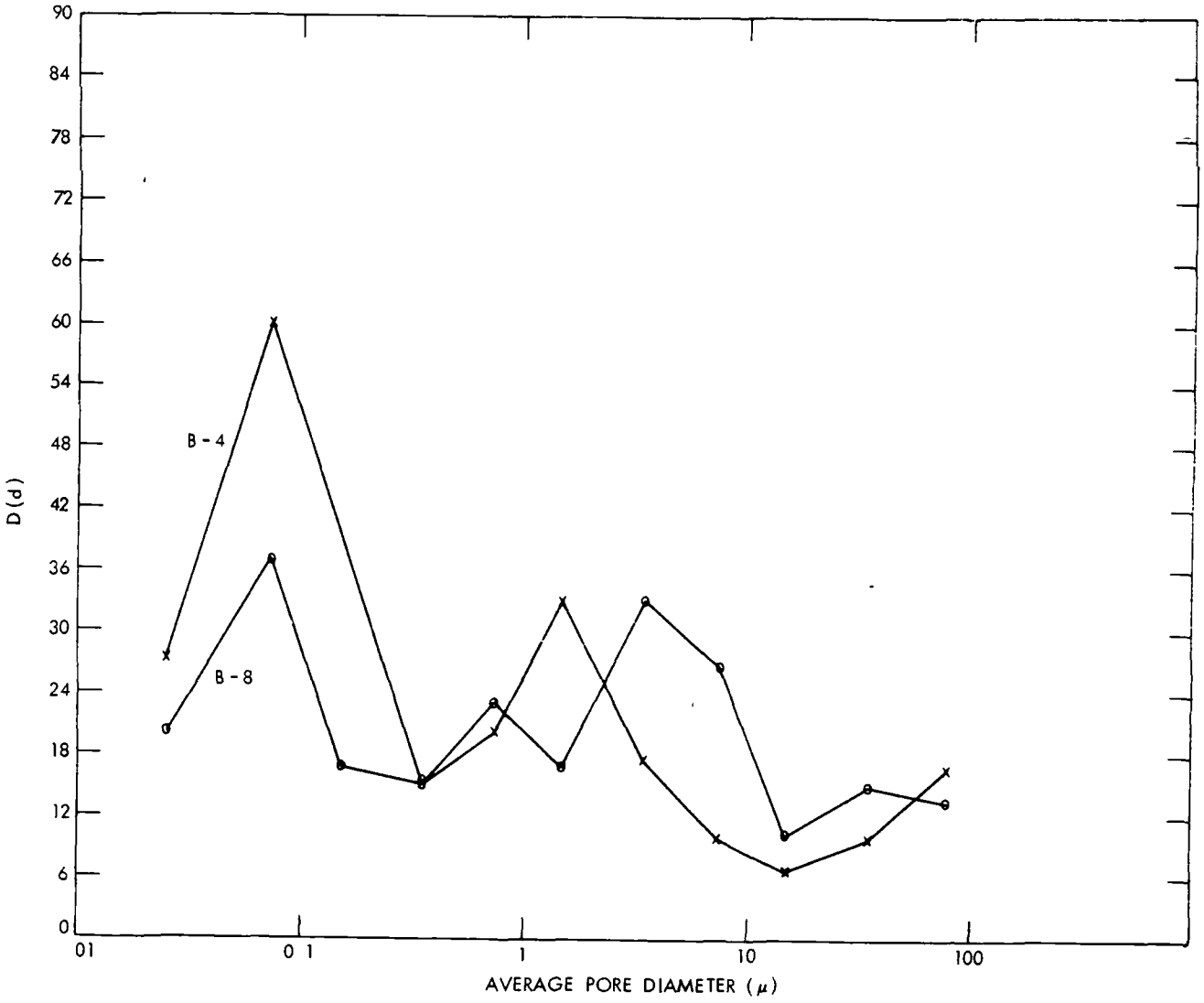

Figure 7f. Pore Size Distribution— Battery 12

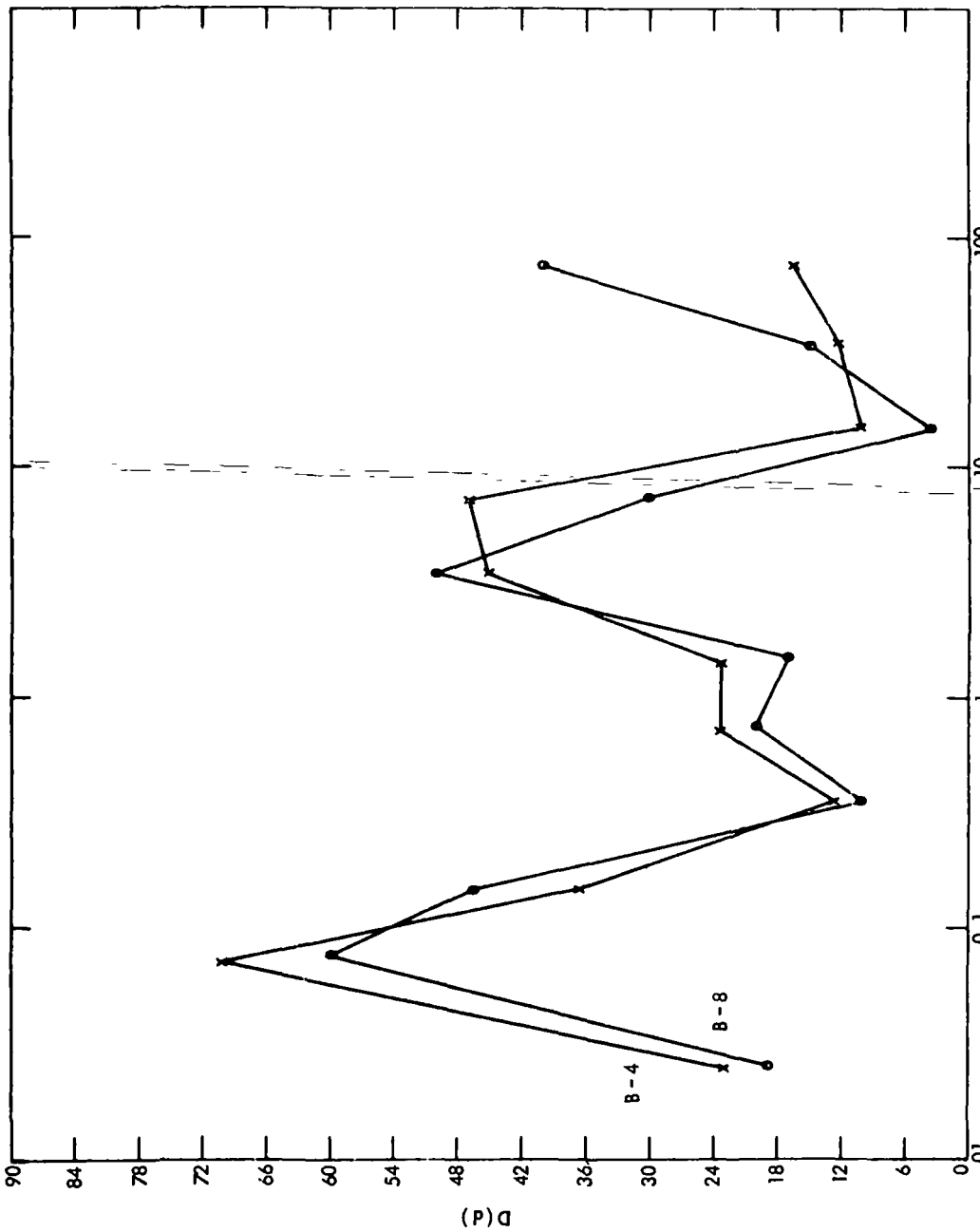

Figure 7g. Pore Size Distribution— Battery 13

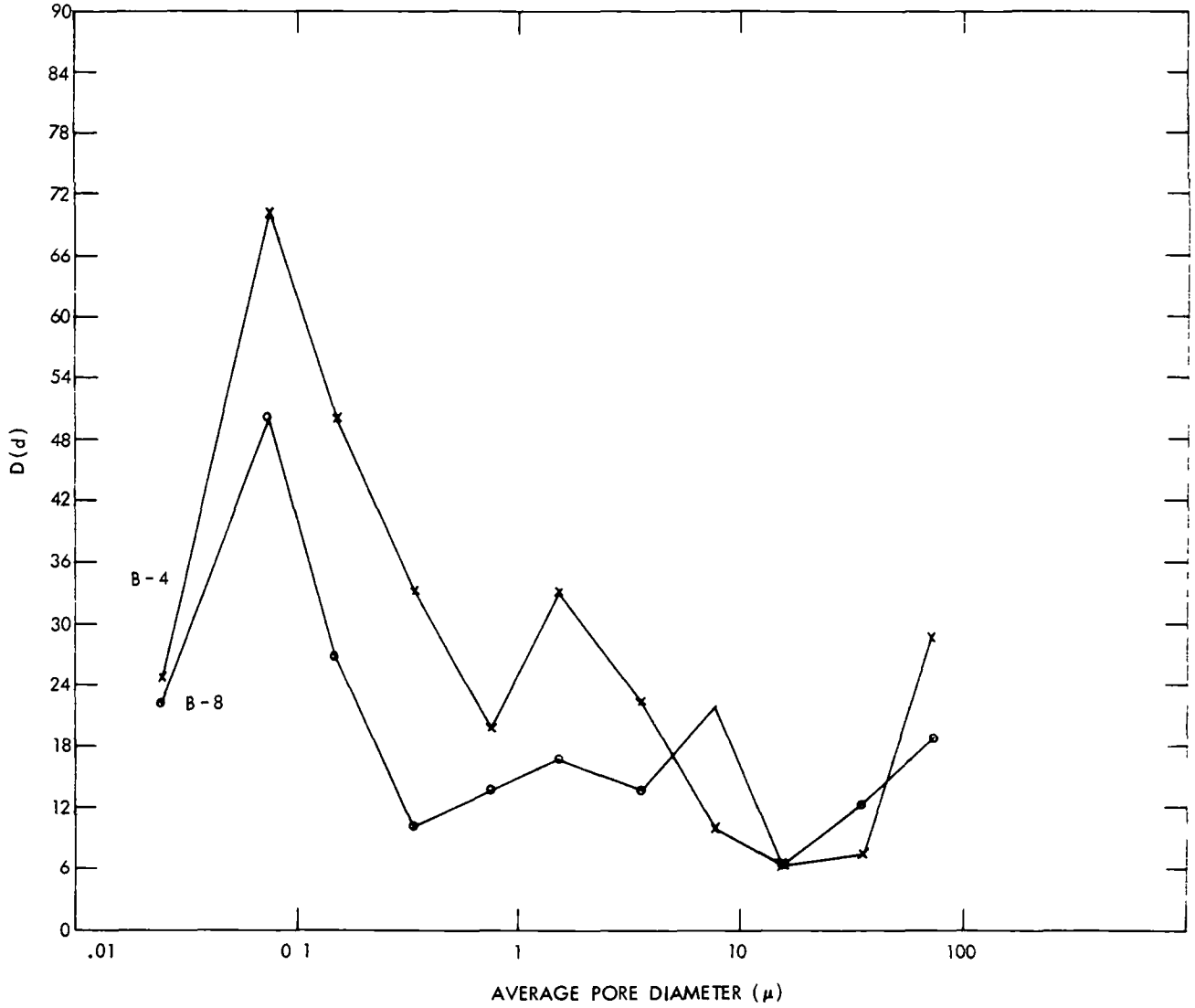

Figure 7h. Pore Size Distribution— Battery 14

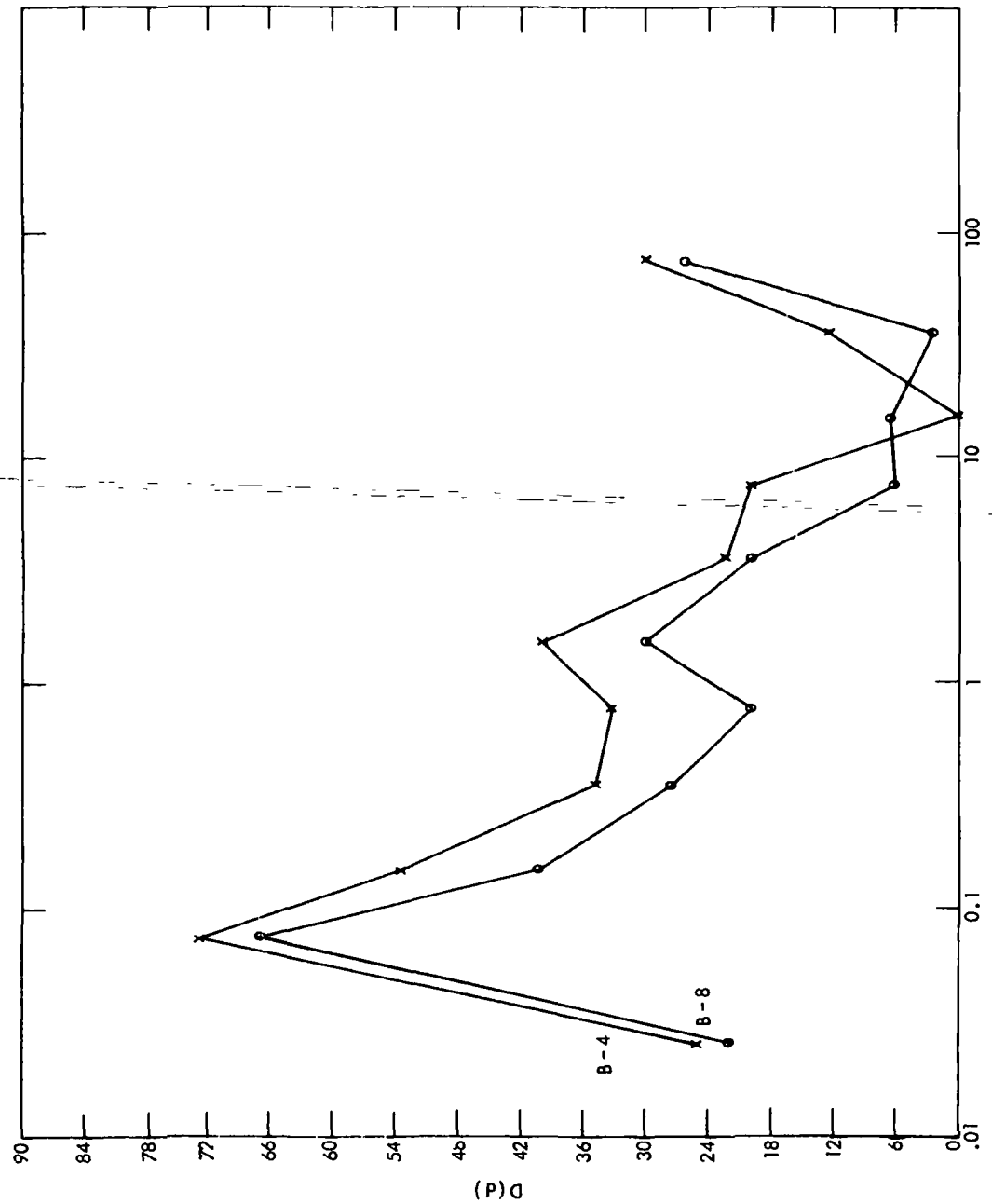

Figure 7i. Pore Size Distribution— Battery 7

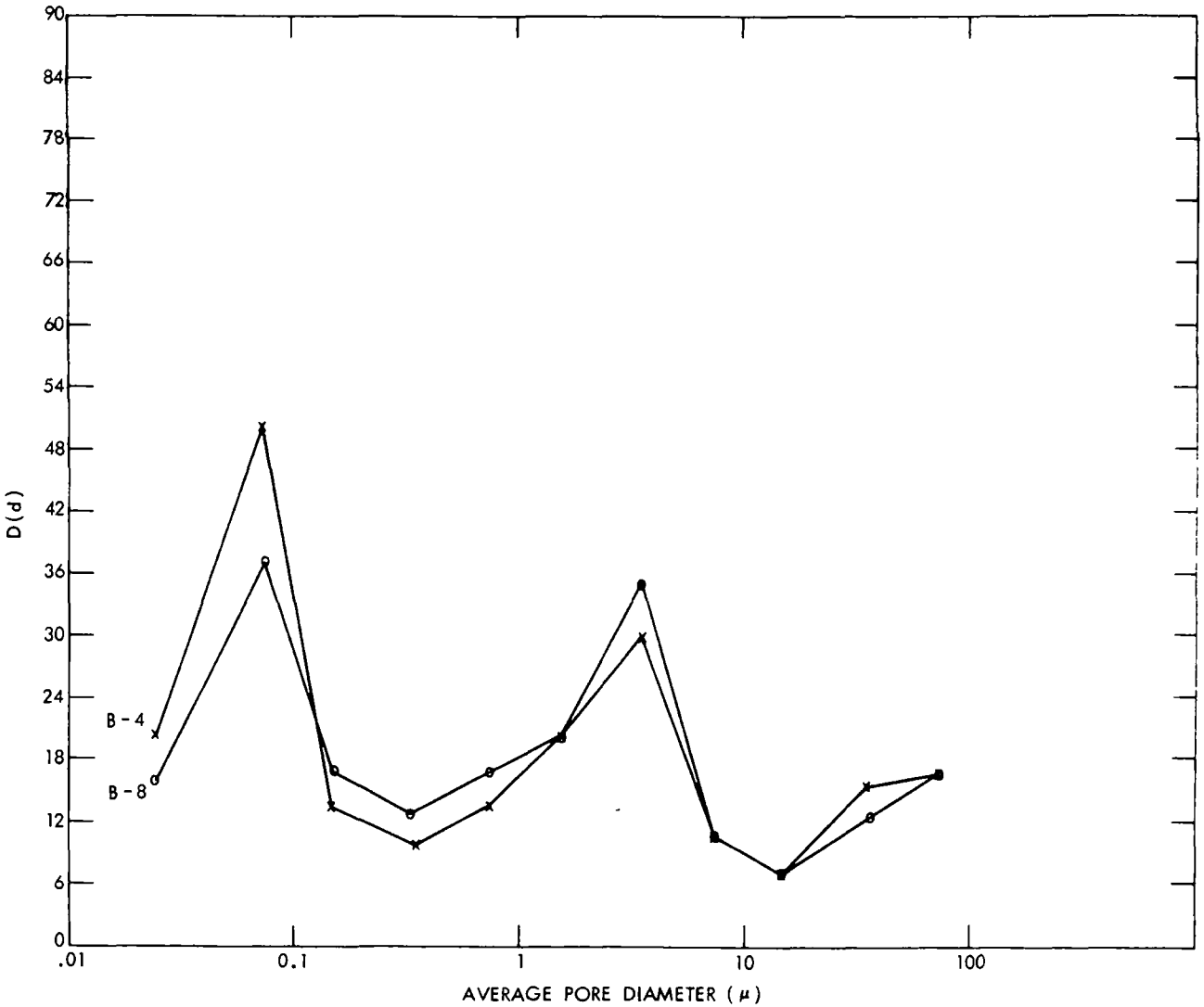

Figure 7j. Pore Size Distribution— Battery 8A

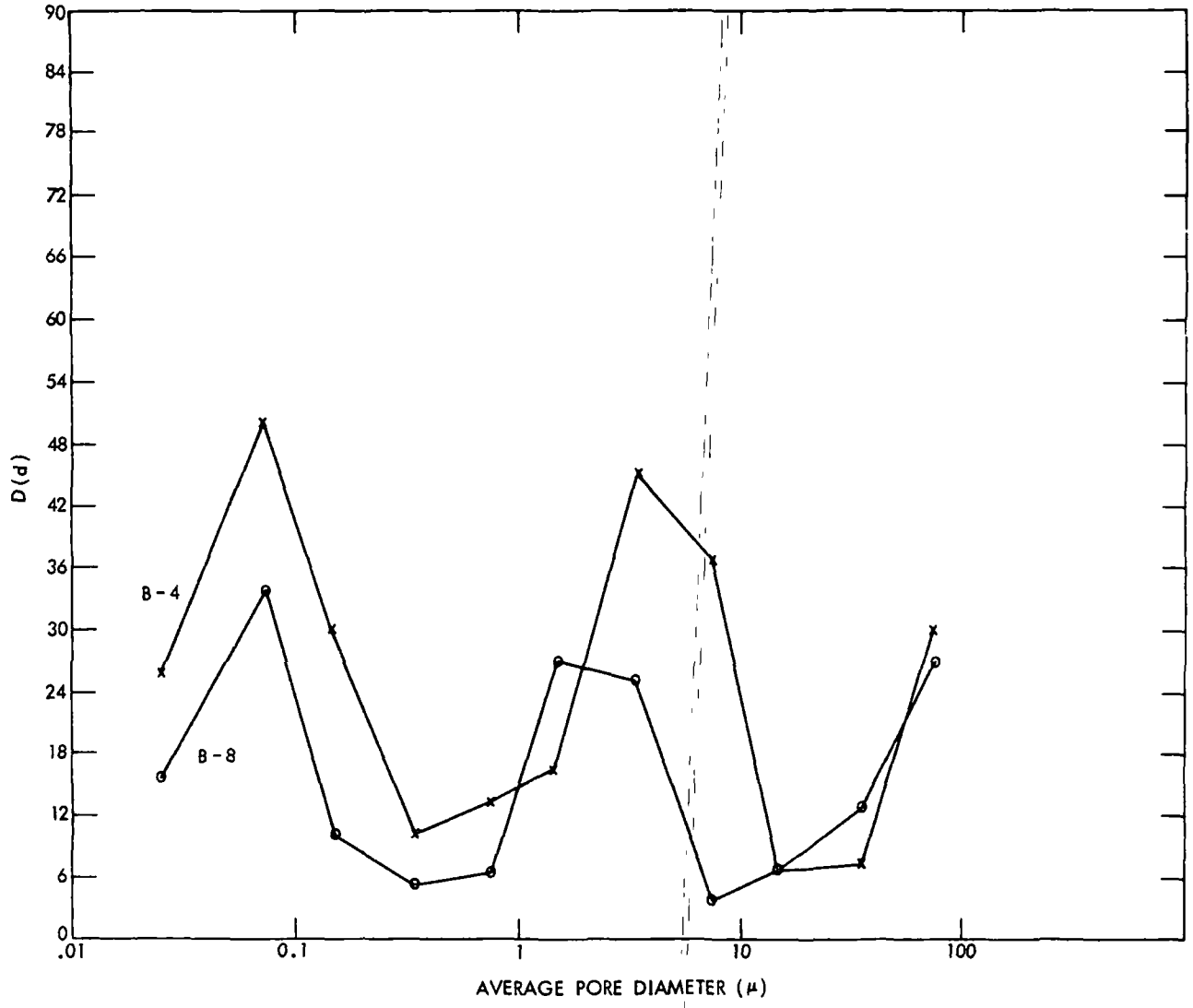

Figure 7k. Pore Size Distribution— Battery 8B

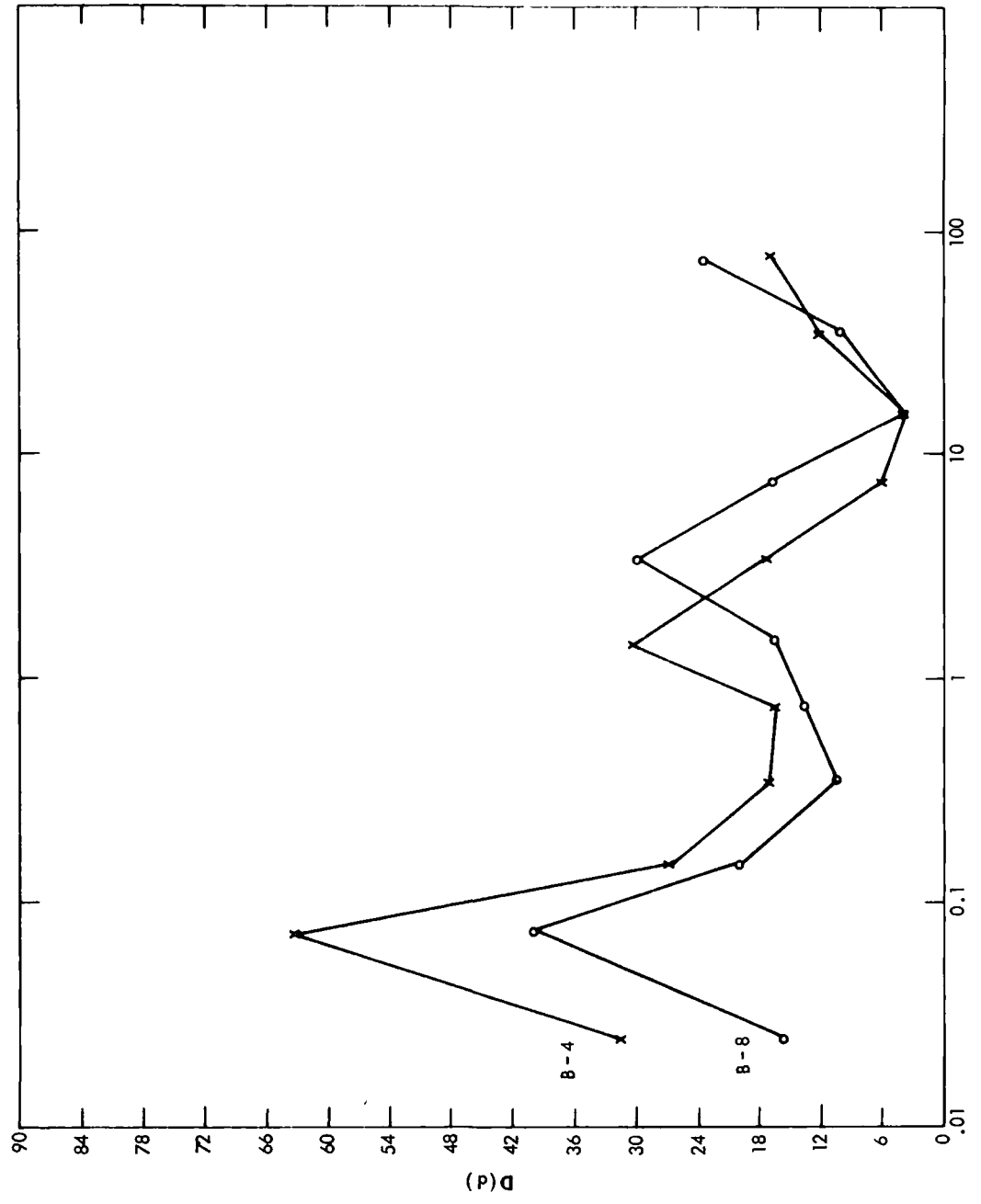

Figure 74. Pore Size Distribution— Battery 9

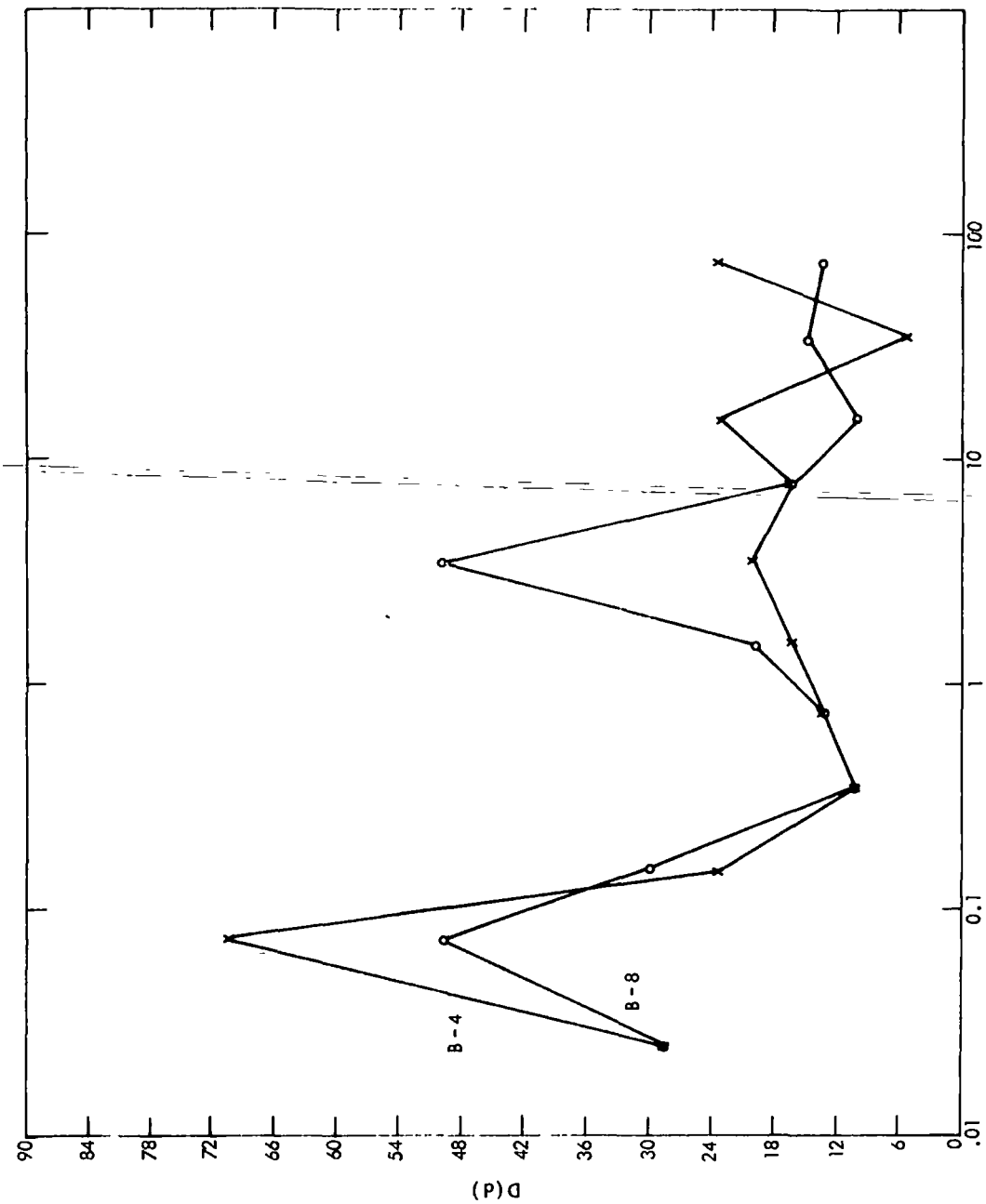

Figure 7m. Pore Size Distribution—Battery 10

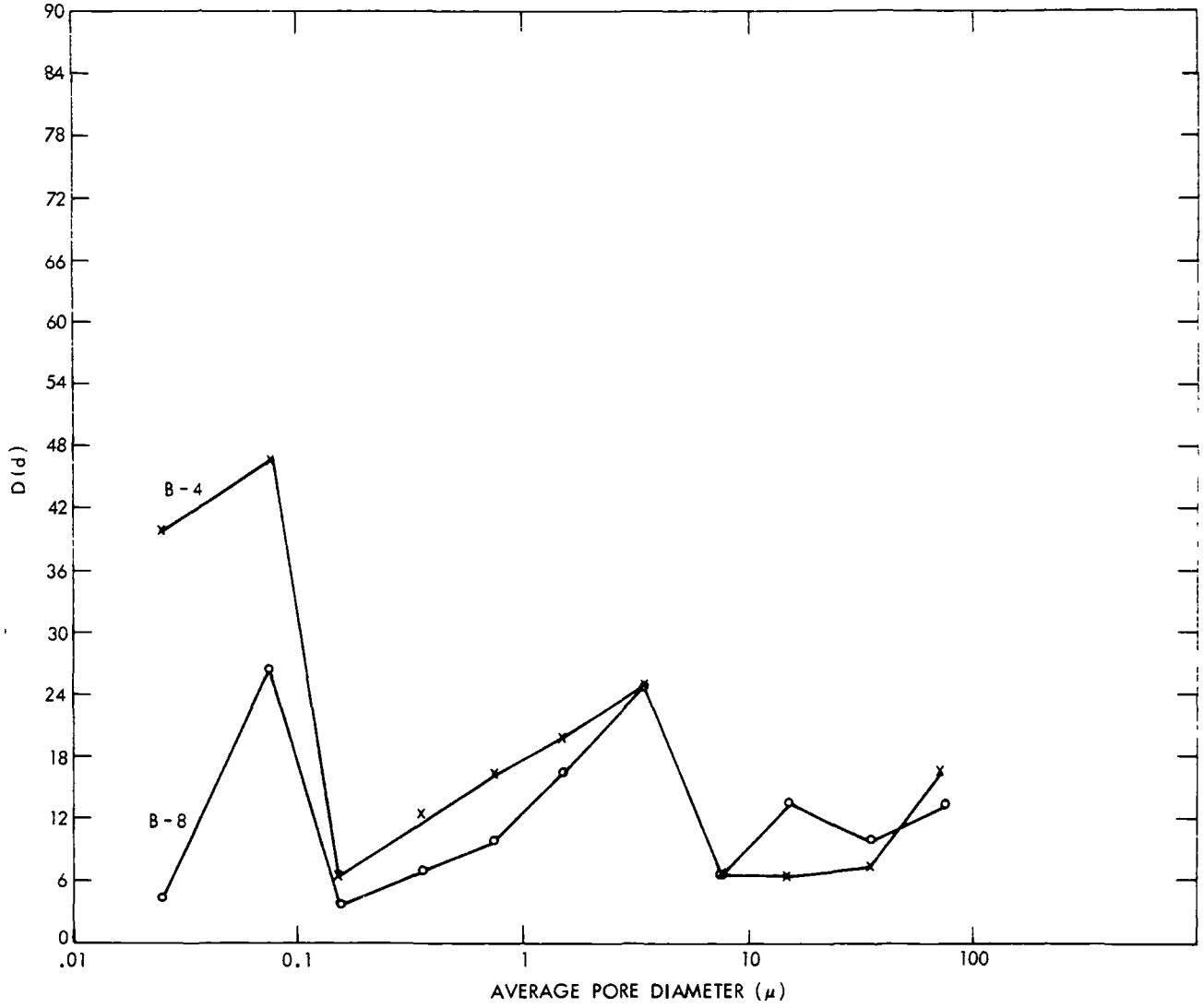

Figure 7n. Pore Size Distribution— Battery 11

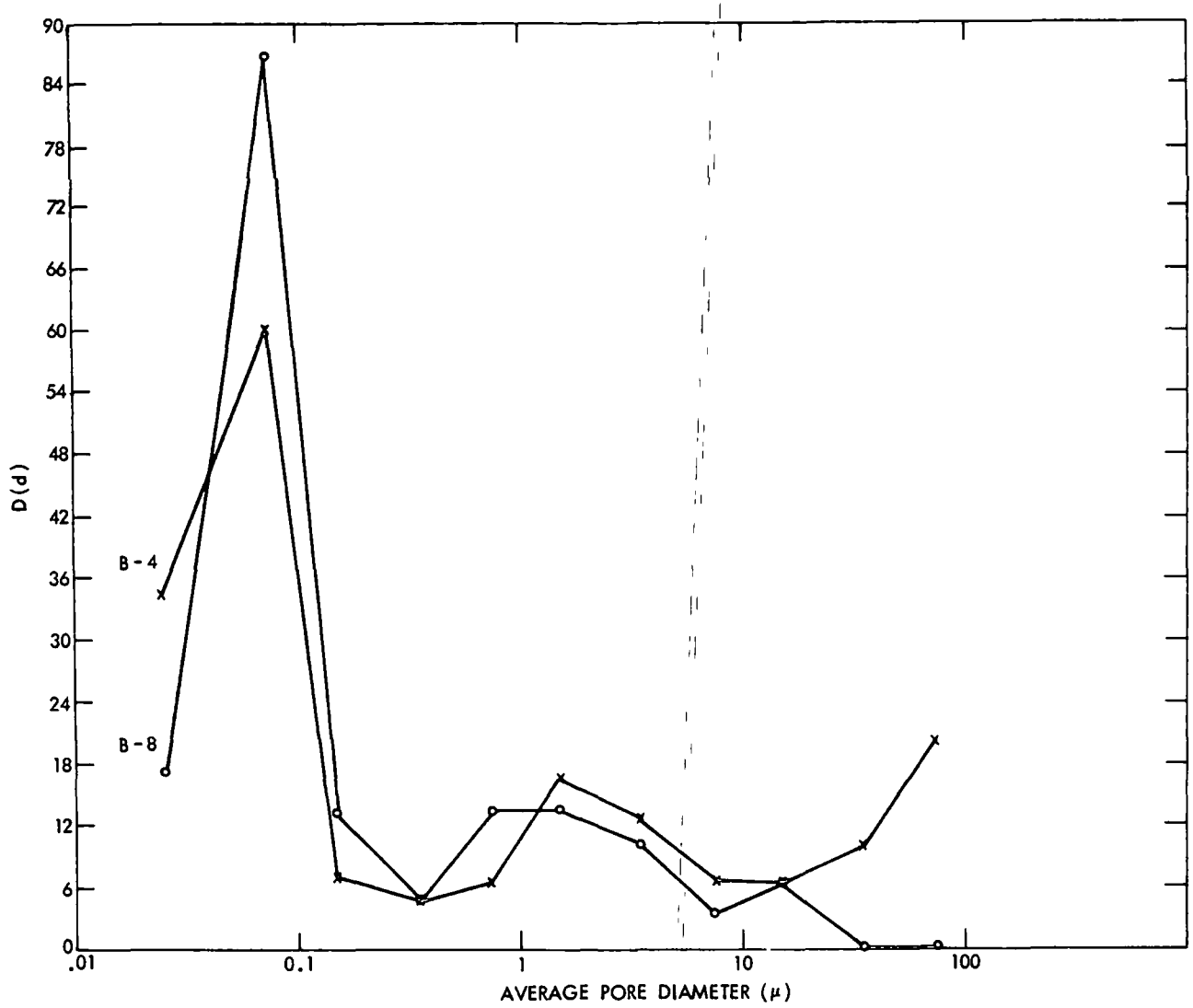

Figure 7o. Pore Size Distribution— Battery AMF 25°

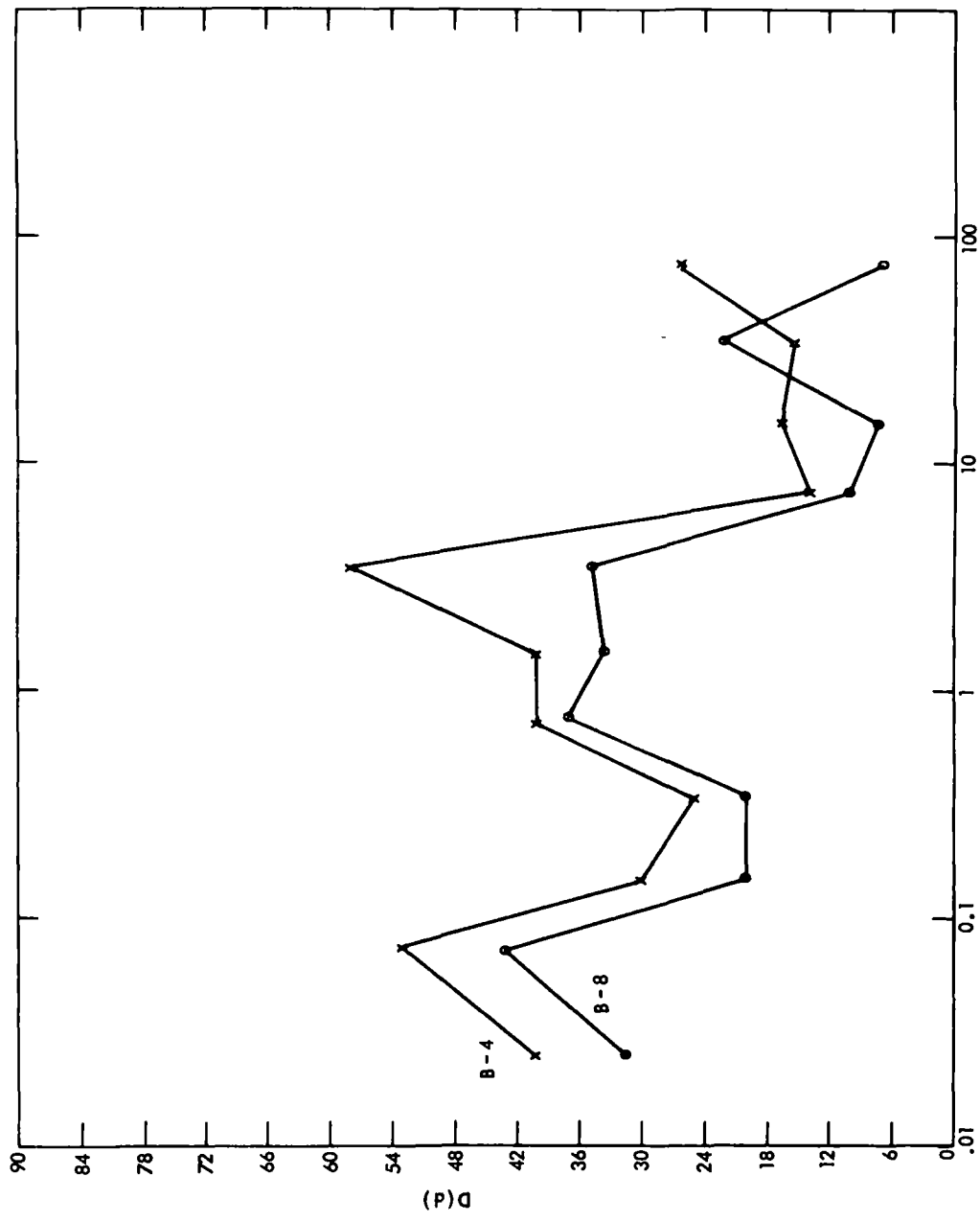

Figure 7p. Pore Size Distribution— Battery AMF 10°

where p is the pressure, d is the diameter, and $\frac{dV}{d(\log d)}$ is the change in volume as the log of the diameter changes. The data are summarized in Table 14.

From the table it can be seen that the most frequent pore size found was of the order of .075 microns. This was true for at least one plate in 15 of the 16 batteries analyzed. In the control battery plates, the most frequent pore sizes were .75 and 75 microns, which are, respectively, 10 and 1,000 times the diameter found on the other plates.

Metallurgical Reduction—To determine what effect the operation of a cell had on the active material, the B-10 plates (one from each battery) were subjected to metallurgical reduction to elemental nickel. This was done by heating a weighed electrode in a reducing atmosphere of dissociated ammonia at a temperature of 800° C for 30 minutes. The cooled electrode was then weighed and the loss of weight used to calculate the amount of active material. The results appear in Table 15.

Table 15

Metallurgical Reduction of Plate B-10

Battery	Initial Weight (A)	After Reduction (B)	Weight Loss (C)	% Loss (C)/(A)	% Active Material
Control	8.5917	6.7810	1.8107	21.1	57.6
0	8.3622	6.6238	1.7384	20.8	56.7
1	9.1500	7.1708	1.9792	21.6	59.0
2	8.6213	6.8266	1.7949	20.8	56.8
4	8.4239	6.5312	1.8927	22.5	61.4
12	8.0481	6.3771	1.6710	20.8	56.8
13	8.1262	6.3866	1.7396	21.4	58.5
14	7.9918	6.3446	1.6472	20.6	56.2
7	8.0586	6.3774	1.6812	20.9	57.0
8A	7.6082	6.0175	1.5907	20.9	57.1
8B	8.0577	6.3529	1.7048	21.2	57.8
9	7.5946	5.9665	1.6281	21.5	58.7
10	8.6747	6.7150	1.9597	22.6	61.8
11	8.3278	6.3238	2.0040	24.1	65.7
AMF 25°	8.6065	6.4941	2.1124	24.5	67.0
AMF 10°	7.9788	6.3631	1.6157	20.2	55.2
Average				21.6	59.0

The process reduces the plate to elemental nickel. The loss in weight is due largely to the conversion of hydroxides of nickel. The loss in weight ranges from 20.2% to 24.5%. Assuming the loss to be due to nickel hydroxide, active material in the plates ranges between 55.2% and 67.0%. It is interesting to note that the largest percentage weight loss was exhibited by a plate from a cell that was operated at 58% depth of discharge in the UDC test cycle (see Figure 1), while the smallest was exhibited by a plate from a cell operated in the identical manner but at 10° C. In the absence of a statistically adequate sample, few if any conclusions can be drawn from these data.

Spectrochemical Analysis—A spectrographic semi-quantitative procedure was used with particular attention to the elements iron, cobalt, zinc, copper, and silver.

The material to be analyzed was removed from the perforated sheet by flexing and bending the plate until the material flaked off. An accurately weighed portion of the material (about one gram) and an identical weight of graphite were thoroughly mixed.

The interpretation of the spectrographic data obtained was done according to established standard spectrographic procedure, which makes use of emulsion calibration and internal standards. The general method is described in many sources. One available and very good discussion is in Reference 10. The detected elements are listed in Table 16.

The development of suitable standards and sample preparation techniques produced a good semi-quantitative analysis for Fe, Co, Zn, Cu, and Ag in the samples.

Examination of the data shows that there is little correspondence between the positive and negative plates of the same group with respect to Fe and Cu; therefore, it appears that neither of these ions has migrated. Zn and Co appear only in the positive plates. Ag was first detected in the negative plates and increased in concentration to a maximum of 1.7 ppm in the negative plate of Battery 9. The increase in silver concentration is directly related to the order in which the samples were removed and sent for analysis. Although silver appears in greater amounts in the latest batteries, no ion migration is evident, because both positives and negatives show increases. The silver has apparently come from the silver braze at the ceramic-metal seal.

Because the chemical analysis is semi-quantitative, the significant differences among the groups of plates for the following elements would be as follows:

Iron—The negative plates have significantly less iron than the positives (an average of 69 ppm vs 162 ppm). The positive plate with the lowest iron is the control battery plate, which was subjected to the least cycling. The iron may be coming from the nickel-plated perforated steel sheet.

Cobalt—Cobalt is present in the positive plates to the extent of approximately 2%.

Zinc—Zinc was detected only in the positive plates, a result which would seem strange; since in silver-zinc cells the zinc forms dendrites, and migrates with ease.

Table 16

Spectrochemical Analysis of Positive and Negative Plates

Chemical Analysis*		Positive Plates Elemental Concentration					Negative Plates		
Battery	Order of Analysis	Fe ppm	Zn ppm	Cu ppm	Ag ppm	Co %	Fe ppm	Cu ppm	Ag ppm
Control	1	80	550	50	nd	1.6	48	50	d
0	2	150	525	150	nd	2.0	52	75	d
1	12	240	600	72	d	2.2	100	46	1
2	3	190	370	105	d	2.0	70	95	1
4	9	160	365	25	d	2.2	35	30	1
12	14	160	450	26	1.0	1.7	75	30	1.5
13	13	175	310	87	d	2.0	70	55	1
14	11	140	620	30	d	1.6	85	55	1
7	10	150	540	60	d	2.0	45	50	1
8A	8	180	310	57	d	2.0	55	52	1
8B	16	145	560	25	1.0	1.6	80	55	1.5
9	15	210	460	70	1.0	2.1	115	86	1.7
10	7	135	500	29	d	1.4	105	52	1
11	5	165	475	30	d	1.8	50	100	1
AMF 10°	6	155	410	35	d	1.5	90	40	1
AMF 25°	4	160	450	105	d	2.0	25	55	1
Average		162	468	60		1.9	69	58	

* Limits of detection: Co, 1 ppm; Zn, 100 ppm; Ag, 0.5 ppm; nd, not detected, d, slightly above detection level.

Copper—Copper was present in both positives and negatives over a range from 25 to 150 ppm with no definite pattern. It probably came from the brass fittings attached to the pressure gauge.

Silver—The concentration of silver on both the positive and negative plates increased in the order in which the samples were sent for analysis. It is presumed that the silver came from the silver braze in the ceramic-to-metal seal and, being lower than 2 ppm, had little effect on the operation.

Differential Thermal Analysis—Positive plate B-4 and negative plate B-7 of each battery were subjected to differential thermal analysis (DTA). The instrument used was the Du Pont Model 900 Differential Thermal Analyzer. Each sample consisted of active and sintered particles flaked off the perforated steel matrix. Each sample, weighing approximately 4 mg, was inserted into a melting-point capillary tube. Glass beads were inserted into a second capillary tube. Matched Chromel Alumel thermocouples were placed into the capillaries with the samples. The capillary tubes together with sample and thermocouple were placed into a heating block, and the temperature was increased at the rate of 20° C per minute. The differences in temperature between the inert glass beads and cell plate material were plotted directly vs temperature. The results have been combined for the 16 battery groups and are summarized in Tables 17 and 18 and Figure 8.

For the positive electrodes, the one endothermic peak which consistently appears as the target is at approximately 300° C, indicative of the $Ni(OH)_2$ peak. Reference 11 describes a peak at 125° C which was indicative of the charged phase. Remembering that the cells were all removed from test at the end of the normal discharge of 25%, there still appears to be a slight hump in the control battery and Batteries 0, 2, 4, 7, and 12 near the 125° C level. It is interesting to note that the materials from Batteries 10 and 11, which were discharged to 1.0v on every cycle, contained the largest peak at 300° C, which is indicative of the discharged state. There appears to be an unusual peak at about 250° C, which is unexplained.

The negative plates exhibit an endothermic curve at approximately 250° C, which is indicative of the decomposition of cadmium hydroxide. Reference 11 suggests that the peak at 320° C may be due to KNO_3 contamination. Notice that the materials from Battery 13 appear to be discharged (most $Cd(OH)_2$) and those from Battery 7 appear to be charged (least $Cd(OH)_2$).

Table 17

Differential Thermal Analysis of Positive Plates

Battery	Weight (mg)	Peaks °C		Normalized Area Under 315°C Peak	Peak Height (Units)
Control	3.9	283	314	164	32
0	3.4	269	299	72	12
1	4.0	269	304	136	20
2	3.9	228	299	148	15
4	3.7	260	314	170	22
12	4.1	242	299	187	27
13	4.0	267	299	95	14
14	3.8	256	290	135	14
7	3.5	240	292	149	7
8A	8.4	-	306	194	21
8B	3.9	-	306	185	23
9	3.2	262	296	153	20
10	4.0	-	308	170	28
11	3.8	290	313	274	99
AMF 25°	3.5	245	324	250	33
AMF 10°	3.5	-	317	193	17
Average				167	25

Table 18

Differential Thermal Analysis of Negative Plates

Battery	Weight (mg)	Peaks °C		Normalized Area Under 256° C Peak	Peak Height (Units)
Control	3.4	256	313	77	19
0	3.9	241	335	88	14
1	4.4	254	317	38	5
2	4.1	258	-	22	8
4	3.9	247	319	49	14
12	4.0	254	319	44	19
13	4.3	250	319	125	>50
14	3.8	256	<316	69	22
7	3.8	246	-	6	1
8A	4.1	255	319	55	16
8B	3.7	248	322	42	8
9	4.0	254	319	48	14
10	4.5	254	317	38	11
11	4.3	255	318	11	5
AMF 25°	3.9	257	317, 391	35	11
AMF 10°	3.8	253	319	28	7
Average				48	14

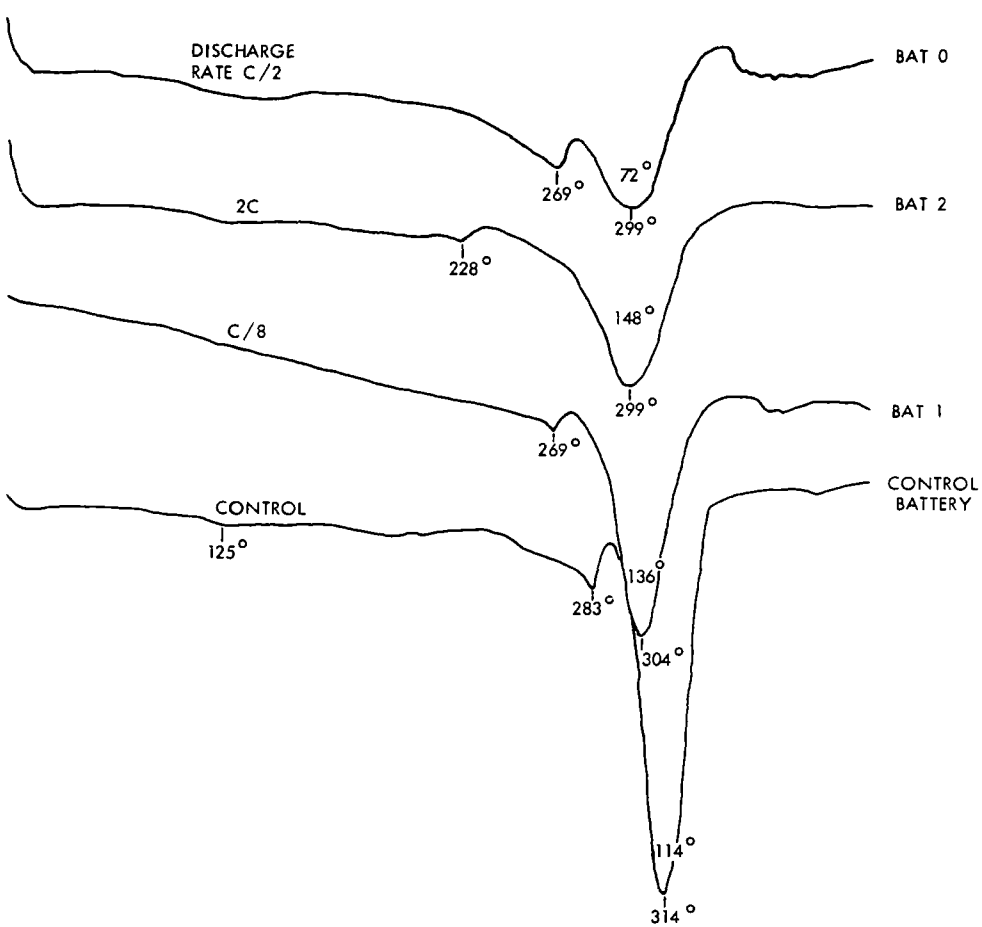

Figure 8a. Differential Thermal Analysis — Positive Plates

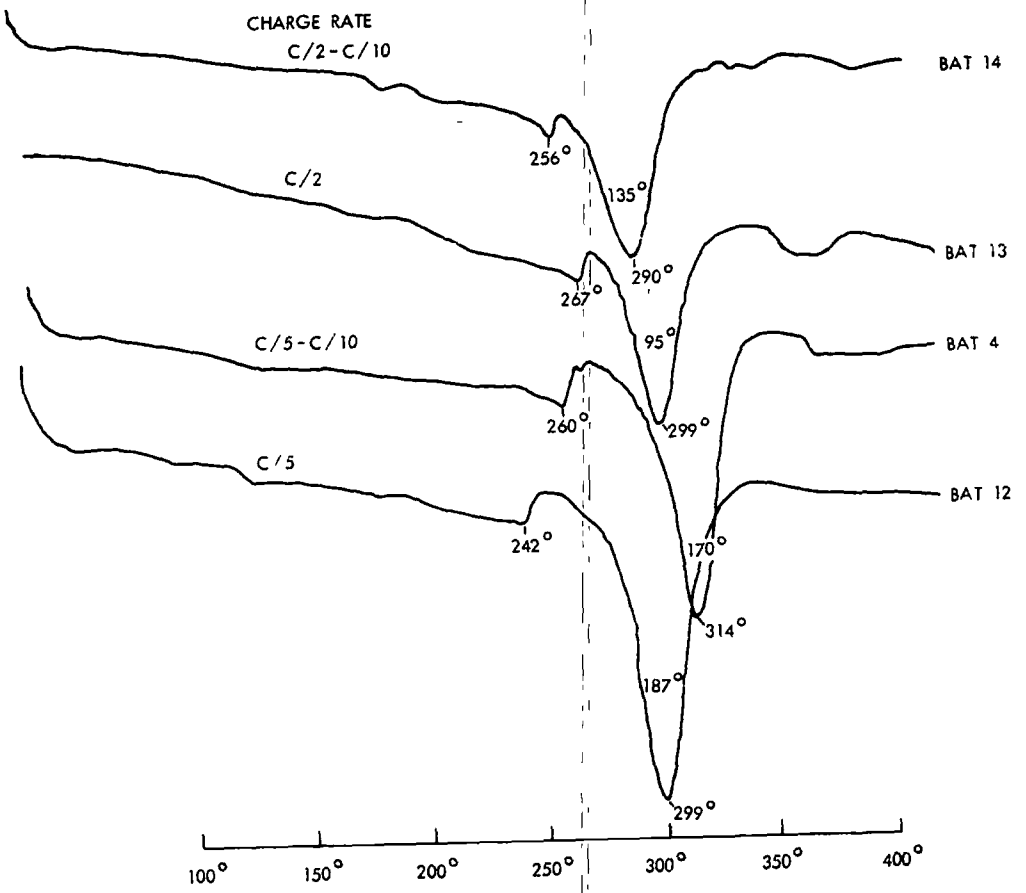

Figure 8b. Differential Thermal Analysis — Positive Plates

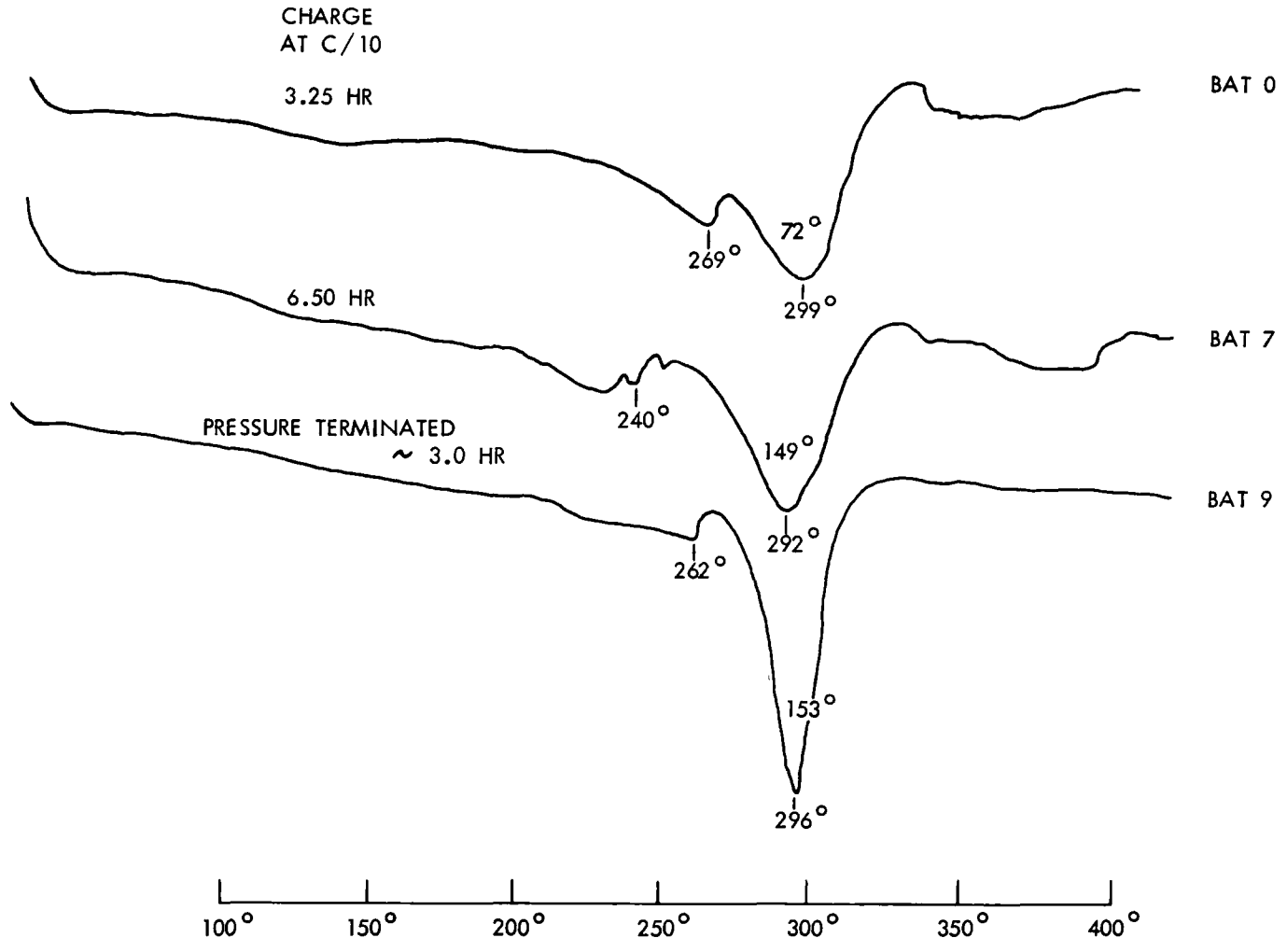

Figure 8c. Differential Thermal Analysis — Positive Plates

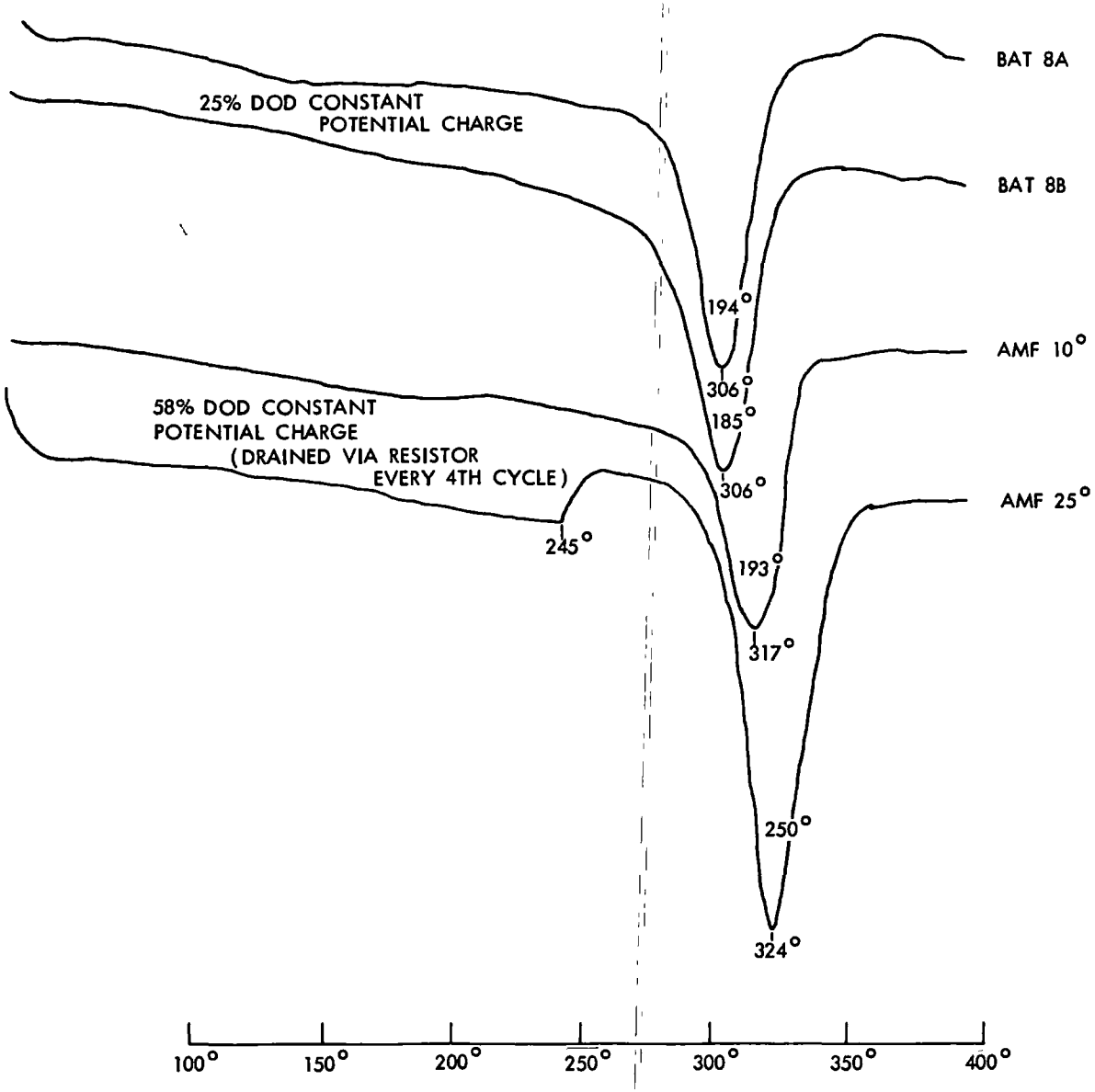

Figure 8d. Differential Thermal Analysis — Positive Plates

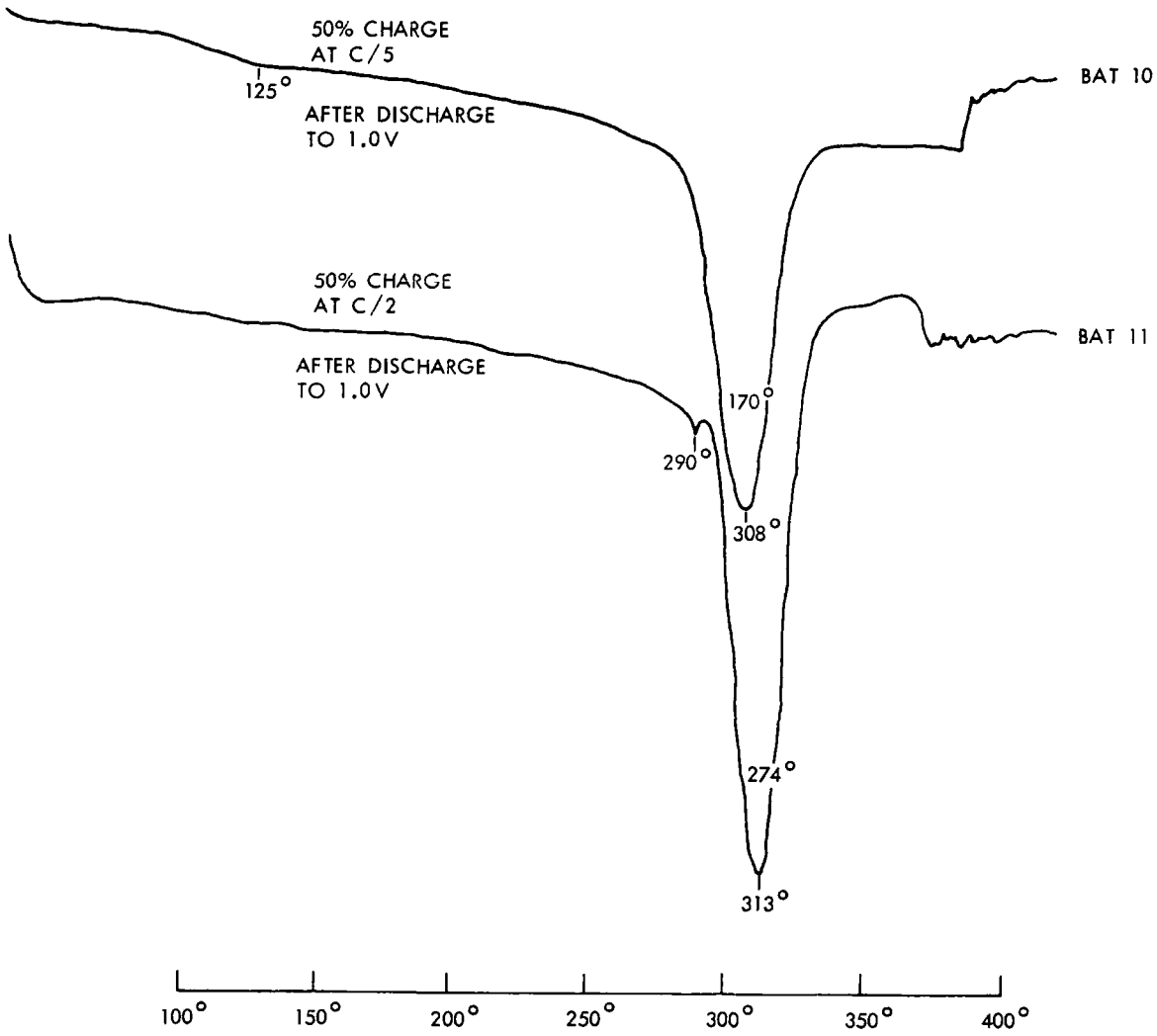

Figure 8e. Differential Thermal Analysis — Positive Plates

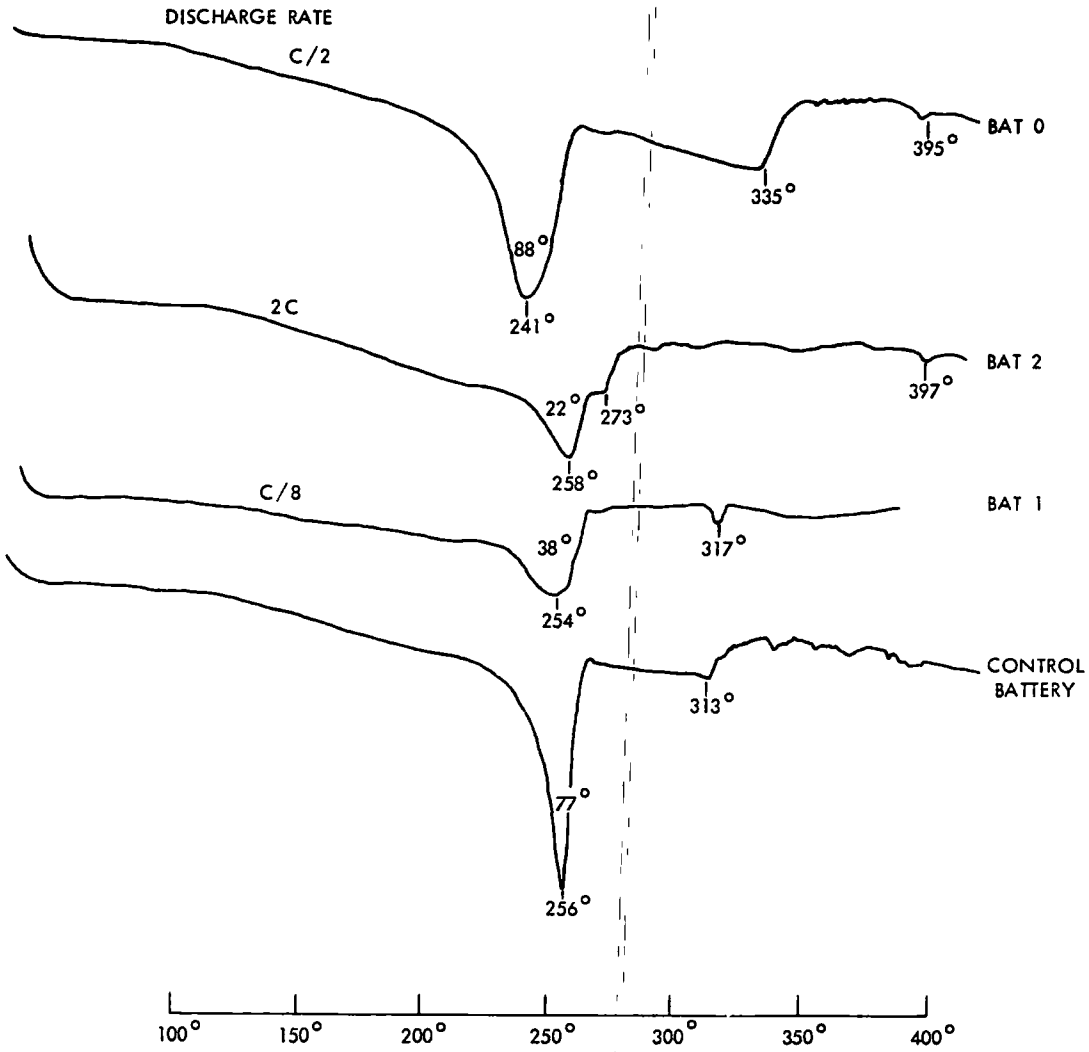

Figure 8f. Differential Thermal Analysis — Negative Plates

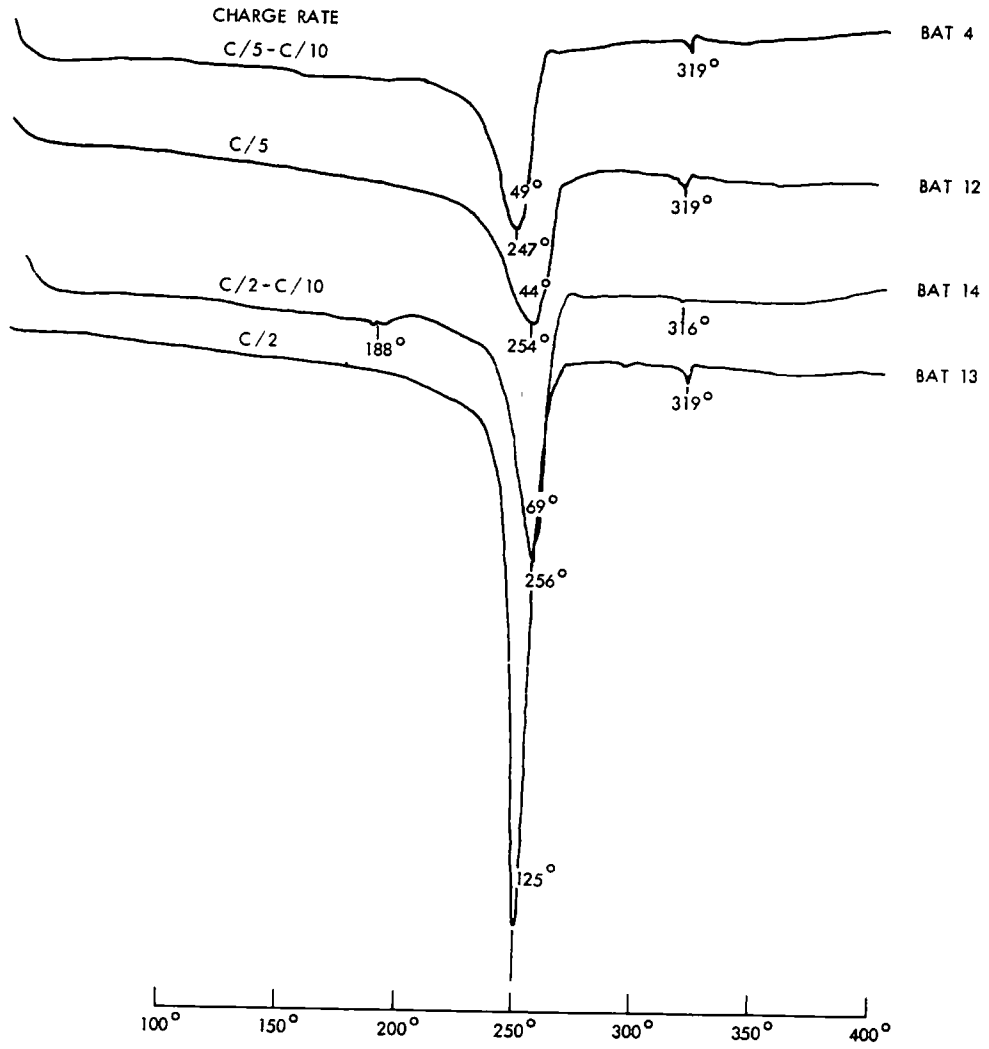

Figure 8g. Differential Thermal Analysis — Negative Plates

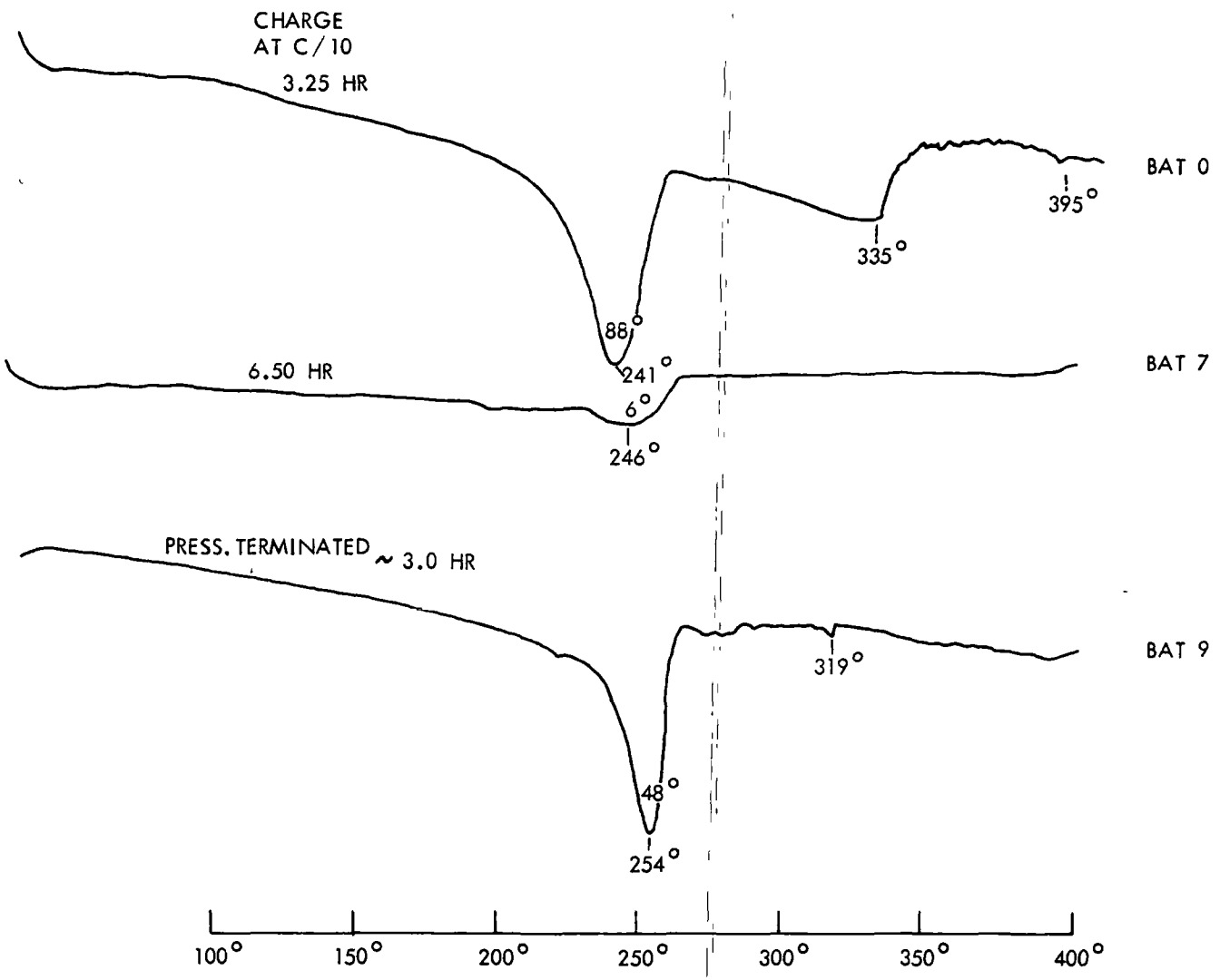

Figure 8h. Differential Thermal Analysis — Negative Plates

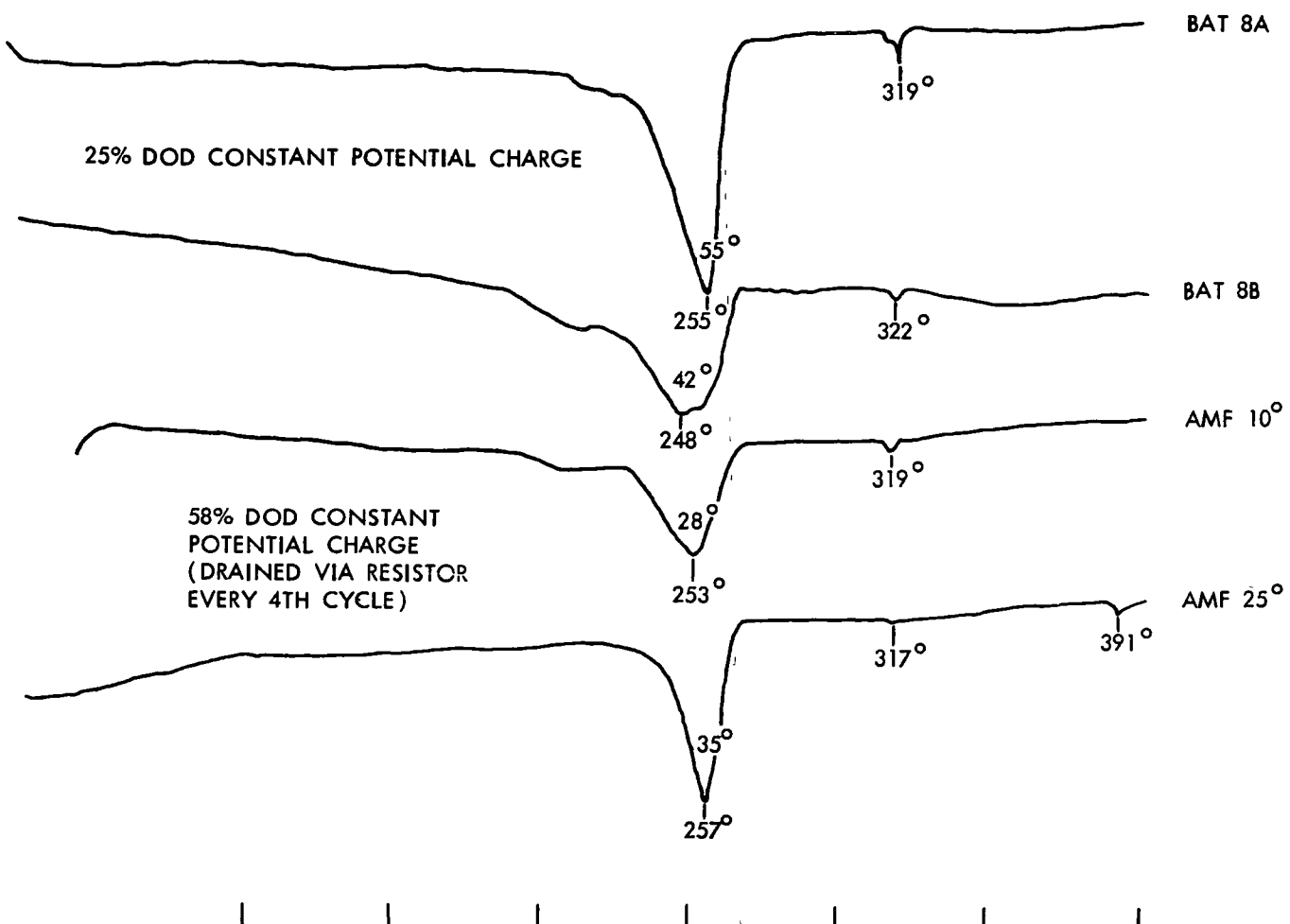

Figure 8i. Differential Thermal Analysis — Negative Plates

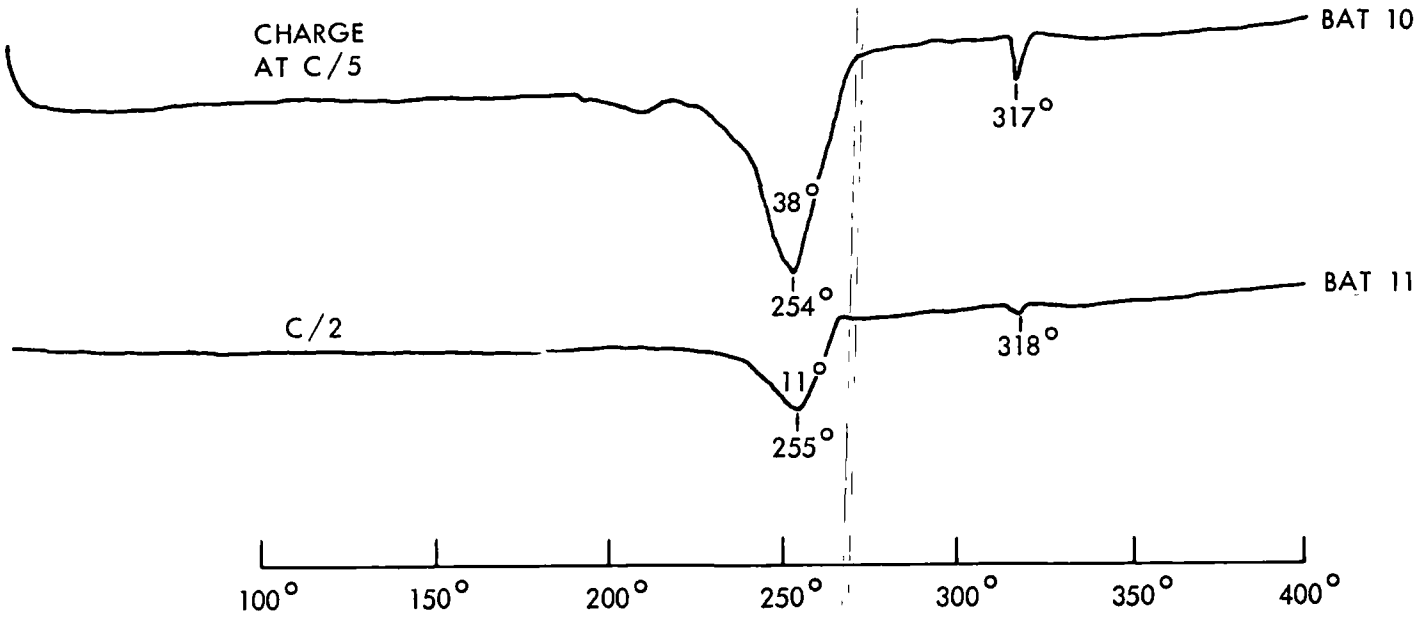

Figure 8j. Differential Thermal Analysis — Negative Plates

Cell Tests

The remaining three "live" cells (C, D, and E—see Figure 2) were each subjected to tests as a cell unit. The purpose of the tests was to determine (a) which electrode failed first and by how much, (b) the oxygen recombination rate and capacity left in the negative electrode, and (c) the steady-state voltage and pressure during overcharge. These tests were performed starting with the cell in the condition found at the end of the normal charge or discharge.

In order to sample the gas within the cell or make measurements of total oxygen recombination, a means had to be provided for entering the cell. Fortunately, many of the cells in the battery cycling test were equipped with pressure gauges. In most cases, three of the remaining five "live" cells had pressure gauges attached. The pressure gauges were attached to the cell via a brass "tee" fitting.

A valve which was always closed during operation of the cells was connected to the third arm of the "tee." However, the valve made it convenient to connect the cell to the sample system of the gas chromatograph used in the gas analysis or to connect to an oxygen tank for studying oxygen recombination rates.

The steady-state voltage and pressure test was terminated when it was decided that it was providing no useful information.

The test and results are described in the next two subsections.

Discharge to Failure—Cell C was the third in the group of five cells from each battery involved in the test program outlined in Figure 1. Cell C was removed from the computer-operated battery test in the charged condition and sent to the analytical laboratory. The cell was connected electrically to a power supply for discharge. A sample chamber of less than 1-cc volume with valve was attached to the valve on the cell. The sample chamber was in turn connected to the gas chromatograph. The valve and tubing arrangement to the gas chromatograph was checked for leaks with helium, then pumped down to vacuum. A Perkin-Elmer Model 154-D gas chromatograph was used for the measurements. The 2-meter-long column consisted of a synthetic zeolite "Molecular Sieve" which readily separates H_2, O_2, and N_2. The thermal conductivity of the sample gas is compared to the conductivity of the carrier gas, namely, helium or argon.

There was approximately a one-hour open-circuit stand between the end of charge and the beginning of discharge. The discharge rate for cell C was the same as that given the cell in the battery test. Voltage and current were monitored during the discharge. When the voltage of the cell dropped to 1.0v, a 1-cc gas sample was extracted from the cell and analyzed in the gas chromatograph. The discharge continued without interruption. When the voltage of the cell had leveled off at -1.0v to -.4v, another sample was taken to determine which electrode had failed first. Two additional samples were taken to confirm the gas composition, and the discharge continued until the voltage dropped to -1.0v, which was considered to be failure of the second electrode.

The data for the test cells have been listed in Table 19. In all test cases, the positive electrode failed first. Notice also that the negative electrode contained a considerable amount of charged material. In the instance of Batteries 10 and 11 and also with a test run on AMF 10°—cells for which the data are unavailable—a strange event occurred. Initially, the discharge to 0.0 volts was similar to that in the other instances, and the voltage leveled off at -.15v. However, as the discharge continued at the 3.1-amp rate, the voltage became slightly more positive, approaching -0.05 volts. Pressure increased slightly, then stopped and actually began to decrease, the discharge continued until 17 ampere hours had been registered. It was suggested that the cell was shorted. To determine whether this was the fact, the cell was given a normal charge of 3.1 ampere hours. It accepted the charge and continued operating for six months in the same Battery 11 cycle mode shown in Figure 1. This unusual occurrence was repeated with another of the Battery 11 cells, also with a Battery 10 cell and with an AMF 10° cell C. Could it have been due to the method of discharging to 1.0 volts on every cycle for the batteries?

The batteries which are missing in Table 19 had no failed cells with pressure gauges on them, or testing was terminated before getting the analysis phase of the program under way. The relationship between oxygen gas recombined and excess negative capacity on neighboring cells is discussed in the next subsection.

Oxygen Recombination—Cell D, also equipped with a pressure gauge and valve, was removed from the battery test at the end of the discharge phase of the cycle in the test program. It was filled (Figure 2) with oxygen gas and the pressure gauge read as the oxygen recombined. When the cell had reached a vacuum condition, it was given another oxygen fill. The rates of recombination are given in Table 20 for cell D of each of the batteries tested. Note that all

Table 19

Overdischarge and Oxygen Recombination Characteristics of Cells C and D

Battery No.	0	1	2	4	7	9	10	11	AMF 25°	AMF 10°
Gulton Group No.	2	12	3	9	10	15	7	5	4	6
ESB Designation	BS	BD	BT	BA	BB	BG	BY	BW	BU	BX
Discharge Current	3.1	.8	12.6	3.1	3.1	3.1	3.1	3.1	6.0	6.0
Ampere Hours to 1.0v	2.1	2.0	1.5	1.5	5.5	1.5	2.8	2.6	2.7	4.0
Rate of Pressure Increase during Overdischarge psi/min/amp	1.1	.63	1.3	.84	1.5	1.0	-	-	-	-
Gas Analysis	H_2	H_2	H_2	H_2	H_2	H_2	H_2	H_2	H_2	H_2
Limiting Electrode	+	+	+	+	+	+	+	+	+	+
Ampere Hours to -1.0v (2nd failure)	5.8	>4.0	5.3	4.7	7.9	3.4	>5.7	>17.0	-	-
Oxygen Recombined (atmospheres)	21.1	Leak	44.9	26.8	63.3	19.3	43.8	20.8	-	-
Equivalent Ampere Hours	2.3	-	5.1	3.1	7.2	2.2	5.0	2.4	-	-
Excess Unaccounted-for Charge in Negative Electrode	3.7	-	3.8	3.2	2.4	1.9	-	-	-	-

cells recombined a relatively large quantity of oxygen, which is the same as saying that the cadmium electrode had a large excess charge when discharged to the battery test discharge end point. In particular, Battery 7 recombined a volume of oxygen equivalent to approximately 7.2 amp hours. This action is consistent with the differential thermal analysis work, which indicated that the electrode contained significantly large quantities of cadmium but little cadmium hydroxide. The large excess charge in the negative is also consistent with the results of the overdischarge tests (see subsection immediately preceding), in which the positive failed first by a considerable amount. The amount of excess charge in the negative electrode found by oxygen recombination and that found by electrically discharging the cell can be compared in Table 19.

Table 20

Rate of Oxygen Recombination (psi/hr)

VO-6HS (26 cc free space)

Fill Battery	0	1	2	4	7	10	11
1	19	26	23	23	30	18	24
2	22	36	23	24	38	16	24
3	21	35	24	25	37	19	21
4	20	Leak	26	24	32	17	15
5	18		22	20	31	17	11
6	12		24	20	32	15	10
7			21	15	30	15	1
8			21	3	28	12	
9			19		27	15	
10			19		28	13	
11			17		24	13	
12			15		25	9	
13			8		25		
14					22		
15					19		
16					20		
17					18		
18					18		
19					15		
20					7		
Total Atmospheres	21.1	-	44.9	26.8	63.3	43.8	20.8
Equivalent Ampere Hours	2.3	-	5.1	3.1	7.2	5.0	2.4

SUMMARY

The influence of operating factors—charge rate, charge termination, discharge rate, etc.—on the life of a nickel-cadmium cell was described in Volume II of the Nickel-Cadmium Battery Test Project. Since the cycle life of a cell depends on the manner in which it is operated, one would expect the operation to influence the physical-chemical characteristics of the cell components, namely, the plates, separators, and electrolyte.

It was the intent of this phase of the test program to analyze the materials from the test cells in order to (a) describe, from an overall view, what the long-term degradative causes of failure were and (b) determine how the degradation was influenced by operating conditions. It must be remembered that the cells subjected to the physical-chemical analysis were those which were still operational ("live") even though five of their neighbor cells in the battery had failed. It was expected that the live cells contained materials which had changed according to the operation given them.

The analysis of the cells and of the materials contained within them was divided into four parts: visual examination, wet chemical analysis, instrumental analysis, and cell tests.

Visual Examination

The visual examination of the electrode pack, including electrodes and separator, gave a clue to the more obvious long-term degradation taking place in the cell. Most cells suffered from separator dryness and strong adhesion of the separator to the negative plate. Although this effect was less pronounced in the first cells analyzed (the control battery and Battery 0), it was quite common in all of the remaining 14 batteries. This condition causes increased impedance, which ultimately results in cell failure. Another visual observation was that the separator, which had strongly adhered to the negative plate, also contained a dark-colored substance. It appeared as if the active material from the negative had grown into the separator. An X-ray diffraction analysis proved that $Cd(OH)_2$ and accompanying unidentified material were imbedded in the separator. This condition produces a high-resistance short between plates which would also cause a reduction in cell life. Both of these conditions could have been worsened by the increased pressure on the electrode plates caused by the shims installed between retainer plate and cell wall on both sides of the can to maintain even pressure on the cell stack when under vacuum or pressure. The plates themselves did not exhibit a shim imprint, although the can wall did.

Other visual observations included a few instances in which material was found on the comb support and instances of coloration of the ceramic seal inside the case.

In the instance of Battery 2, which was operated at a 2C discharge rate, blistering of the positive plates was noted, which is indicative of high-rate discharge.

The results of the wet chemical analysis and instrumental analysis are summarized in Tables 21 to 24 according to battery test group (see Figure 1). Group 1, the comparison of battery discharge rates, is given in Table 21; Group 2, the comparison of battery charge methods, is given in Table 22; Group 3, the comparison of battery charge termination methods, is given in Table 23; and Group 4, the comparison between batteries operated from a completely discharged condition (height of charge) and the AMF batteries, is given in Table 24.

In scanning these data, it is evident that there is as much variation between samples of materials from the same cells as there is between two pairs of cells from the same battery (8A and 8B), which exhibit marked variation. Both types of variation can be noted in the weight analysis, surface area measurement, pore size distribution, and other characteristics. Unfortunately, the variation in materials tends to obscure significant differences between different batteries within a given group or between groups. One explanation for this tendency is that the materials themselves were non-uniform to begin with, a problem which is now being investigated. The five "live" cells removed from a battery and sent for analysis when their neighbors in the same battery failed had reached a point of old age, and although in "operating" condition were actually suffering from the same causes of failure. This is in itself an important finding in that it indicates that the wearout mode for materials from cells operated for prolonged periods is similar regardless of the operating conditions, with the exception of extreme operating methods such as the 2C discharge rate for Battery 2. This battery, which was operated at a high discharge rate, experienced plate blistering. This problem would not normally arise under less strenuous conditions. The results of the wet chemical analysis, instrumental analysis, and cell tests are summarized below in terms of the general effects noted in the degradation process.

Wet Chemical Analysis

As described in the section on wet test methods, the data for the control battery are considered non-random with a 99% confidence. The positive and

PAGE MISSING FROM AVAILABLE VERSION

Table 21

Group 1 Cell Comparisons

		Control Battery	Battery 1	Battery 0	Battery 2
Order of Analysis (in 16 analyses)		1	12	2	3
Cycle—Charge		C/10 for 16 hr	C/10 for 3 25 hr	C/10 for 3 25 hr	C/10 for 3 25 hr
Discharge		C/2 to 1 0v	C/8 for 2 hr	C/2 for 0 5 hr	C/2 for 125 hr
Number of Cycles					
When sent for analysis	4,448 average (of 16)*	9	3,100	3,065	2,072
To failure	4,691 average (of 16)	-	3 928**	3,065	2,072
Visual Inspection					
Cell Thickness Cell A (top - middle - bottom)		812 811 812	812 753 819	803 753 818	803 784 801
Cell B (top - middle - bottom)		814 818 811	809 759 810	812 753 817	801 747 810
Notes		Nothing unusual	Extreme adhesion of separator (both cells)	Nothing unusual	Blistering of plates, heavy adhesion, dendrites at terminals
Wet Chemical Analysis					
Plate Weights w/r to Average					
- As removed	8 00 gm average	+ 01	+ 19	- 13	- 12
- Dry	6 81 gm average	+ 21	+ 02	0	- 01
- Loss/gm	18 gm average	- 04	+ 02	- 02	- 02
+ As removed	9 19 gm average	- 24	+ 19	- 24	- 09
+ Dry	8 25 gm average	- 21	+ 17	- 11	+ 01
+ Loss/gm	11 gm average	0	+ 01	- 01	- 01
KOH Uptake w/r to Average					
-	1 68% average	- 78	+1 19	- 27	- 05
+	96% average	0	- 07	+ 02	+ 12
KOH Titration w/r to Average					
-	29 59 mg/gm average	-5 08	+3 06	-10 07	-3 34
+	27 93 mg/gm average	-6 98	- 20	-9 96	+ 39
Instrumental Analysis					
X-Ray Diffraction—Dry					
-		$Cd(OH)_2$ Ni	$Cd(OH)_2$ Cd Ni	$Cd(OH)_2$ Ni	$Cd(OH)_2$ Ni Cd
+		Ni $Ni(OH)_2$	Ni $Ni(OH)_2$ $CaCO_3$	Ni $Ni(OH)_2$	Ni $Ni(OH)_2$
X-Ray Diffraction					
Discharged		Ni $Ni(OH)_2$	Ni $Ni(OH)_2$	Ni $Ni(OH)_2$	Ni
+ As removed		Ni $Ni(OH)_2$	Ni $Ni(OH)_2$ $CaCO_3$	Ni $Ni(OH)_2$ $Cd(OH)_2$	Ni
Charged		Ni	Ni Cd	Cd Ni $Ni(OH)_2$	Ni
Overcharged		Ni	Ni $CaCO_3$	Ni $Ni(OH)_2$	Ni
Surface Area (m^2)					
-	8 28 m^2 average	6 67 8 65 8 65	<3 <3 6 66	9 52 8 05 6 72	4 12 * 64 6 13
+	170 m^2 average	190 191	156 182	167 159	159 164
Pore Size Distribution (+ plates only), plates B-4 & B-8					
Total porosity	046 cc/gm average	069 047	050 049	047 048	.046 047
Max effective pore diam (μ)	31 6μ average	60 8 27 2	34 40	3 9 5 9	5 9 6 5
Min effective pore diam (μ)	049μ average	051 054	048 048	< 050 050	< 050 054
Greatest number of pores	(units)	75 (76) 75 (30)	075 (66) 075 (64)	075 (70) 3 5 (75)	075 (54) 075 (43)
2nd greatest number of pores	(units	75 (60) 3 5 (18)	3 5 (35) 7 5 (33)	3 5 (35) 075 (60)	1 5 (46) 75 (33)
Metallurgical Reduction (% Active Material) 58 8% average		57 4	58 9	56 6	56 7
Spectrochemical Analysis					
- Fe	69 ppm average	48	100	52	70
- Cu	58 ppm average	50	46	75	95
+ Fe	162 ppm average	80	240	150	190
+ Co	1 9% average	1 6%	2 2%	2 0%	2 0%
+ Zn	468 ppm average	550	600	525	370
+ Cu	60 ppm average	50	72	150	105
Differential Thermal Analysis					
- First Peak (2nd)		256 (313)	254 (317)	241 (335)	258
- Height	14 average	19	5	14	8
- Normalized Area	48 average	77	38	88	22
+ First Peak (2nd)		285 (314)	269 (304)	269 (299)	228 (299)
+ Height	25 average	32	20	12	15
+ Normalized Area	167 average	164	136	72	148
Cell Tests					
Amp hr charge in positive		-	2 0	2 1	1 5
Amp hr charge in negative		-	4 0	5 8	5 3
Oxygen amp hr recombined		-	(leak)	3 7	3.8

*Averages in general are for 16 batteries
**Battery had not yet failed

PAGE MISSING FROM AVAILABLE VERSION

Table 22

Group 2 Cell Comparisons

	Battery 1	Battery 12	Battery 13	Battery 14
Order of Analysis (in 16 analyses)	9	11	11	11
Cycle – Charge Discharge	C/5 to E$_4$ C/10 to E$_1$ C/2 for 0 5 hr	C/5 to 1 125 v C/2 for 0 5 hr	C/2 to 1 150 v C/2 for 0 5 hr	C/2 for 10 min C/10 to 1 42 v C/2 for 0 5 hr
Number of Cycles When Sent for Analysis 4,448 average (of 16)* To Failure 4,691 average	5 418 5 418	4 700 1 021**	5 350 5 970**	1 905 2, 128**
Visual Inspection Cell Thickness Cell A (top-middle-bottom) Cell B (top-middle-bottom)	806 750 801 809 785 818	820 804 820 810 800 82	807 819 809 802 816 807	807 781 811 810 790 816
Notes	Separator adhesion to most negative plates, crystals on positive comb support, ceramic black on inside (both cells)	Nothing unusual	Extreme adhesion to negative plates (one cell)	Strong separator adhesion (both cells)
Wet Chemical Analysis Plate Weights w/r to Average				
– As removed 8 00 gm average – Dry 6 81 gm average – Loss/gm 18 gm average	– 14 – 11 – 01	+ 12 + 11 – 01	+ 47 + 45 – 01	+ 09 + 18 – 03
+ As removed 9 19 gm average + Dry 8 25 gm average + Loss/gm 11 gm average	– 02 + 01 0	– 16 – 44 + 02	+ 20 0 + 01	– 18 – 20 + 01
KOH Uptake w/r to Average – 1 68% average + 96% average	+ 04 – 14	– 12 – 05	+1 23 + 12	+32 – 03
KOH Titration w/r to Average – 29 59 mg/gm average + 27 93 mg/gm average	+1 13 +2 08	+1 79 +2 43	+5 74 +2 86	+2 60 + 38
Instrumental Analysis X-Ray Diffraction— Dry – +	Ni $Cd(OH)_2$ Ni $Ni(OH)_2$ $CaCO_3$	Ni $Cd(OH)_2$ Ni $Ni(OH)_2$ $CaCO_3$	Ni $Cd(OH)_2$ Ni $Ni(OH)_2$ $CaCO_3$	Ni $Cd(OH)_2$ Ni $Ni(OH)_2$ $CaCO_3$
X-Ray Diffraction Discharged + As removed Charged Overcharged	$Ni(OH)_2$ Ni $Ni(OH)_2$ Ni $CaCO_3$ Ni Ni	$Ni(OH)_2$ Ni $Ni(OH)_2$ Ni $Cd(OH)_2$ $Ni(OH)_2$ Ni Ni	$Ni(OH)_2$ Ni $Ni(OH)_2$ Ni $Ni(OH)_2$ Ni $CaCO_3$ Ni	$Ni(OH)_2$ Ni $Ni(OH)_2$ Ni $Ni(OH)_2$ Ni Ni
Surface Area (m^2) – 8 28 m^2 average + 170 m^2 average	15 62 24 07 7 62 156 212	7 09 9 71 8 70 176 160	8 18 8 81 7 02 189 190	8 81 6 81 5 27 190 176
Pore Size Distribution (+ plates only), (plates B-4 & B-8) Total Porosity 046 cc/gm average Max Effective Pore Diam (μ) 31 6μ average Min Effective Pore Diam (μ) 049μ average Greatest Number of Pores (units) 2nd Greatest Number of Pores (units)	048 052 37 12 053 050 3 5 (76) 0 75 (60) 0 75 (73) 7 5 (40)	051 045 19 26 045 049 075 (60) 075 (17) 1 5 (19) 1 5 (8)	056 052 30 55 050 050 075 (70) 075 (60) 7 5 (17) 1 5 (50)	036 056 40 40 045 045 075 (70) 075 (50) 1 5 (13) 7 5 (22)
Metallurgical Reduction (% Active Material) 58 8% average	61 2	56 5	58 1	56 1
Spectrochemical Analysis – Fe 69 ppm average – Cu 58 ppm average	35 30	75 0	70 55	85 55
+ Fe 162 ppm average + Co 1 9% average + Zn 468 ppm average + Cu 60 ppm average	160 2 2 365 25	160 1 7 450 26	175 2 0 710 87	140 1 6 620 40
Differential Thermal Analysis – First Peak (2nd) – Height 14 average – Normalized Area 48 average	247 (319) 14 49	254 (319) 19 44	250 (310) 30 125	256 (316) 22 69
+ First Peak (2nd) + Height 25 average + Normalized Area 167 average	260 (314) 22 170	242 (297) 27 187	267 (299) 11 95	256 (290) 14 135
Cell Tests Amp hr charge in positive Amp hr charge in negative Oxygen amp hr recombined	1 5 4 7 3 2	--- --- ---	--- --- ---	--- --- ---

* Averages in general are for 16 batteries
** Battery had not yet failed

PAGE MISSING FROM AVAILABLE VERSION

Table 23

Group 3 Cell Comparisons

	Battery 7	Battery 8A	Battery 8B	Battery 9
Order of Analysis (in 16 analyses)	10	8	16	15
Cycle - Charge Discharge	C/10 for 6 5 hr C/2 for 0 5 hr	Constant v to C/10 C/2 for 0 5 hr	Constant v to C/10 C/2 for 0 5 hr	C/10 to press cutoff C/2 for 0 5 hr
Number of Cycles When Sent for Analysis 4,448 average (of 16)* To Failure 4,691 average (of 16)	2,300 2,837	8,033 8,500**	9,880 10,218**	4,025 4,582**
Visual Inspection Cell Thickness Cell A (top-middle-bottom) Cell B (top-middle-bottom)	811 767 824 808 731 816	811 752 819 805 739 800	810 780 822 811 751 821	804 765 802 812 729 819
Notes	Crystals on positive comb support ceramic black (one cell)	Separator very moist, adhesion of separator to negative plates (both cells)	Ceramic black, KOH crystals on inside comb support (both cells)	Separator adhesion on plates (both cells)
Wet Chemical Analysis Plate Weights w/r to Average				
- As removed 8 00 gm average	- 16	- 04	+.06	- 05
- Dry 6 81 gm average	- 09	- 17	+ 04	+ 05
- Loss/gm 18 gm average	- 01	+ 03	0	- 02
+ As removed 9 19 gm average	- 31	+ 13	+ 03	- 26
+ Dry 8 25 gm average	-.27	+ 21	+ 07	- 18
+ Loss/gm 11 gm average	+.01	-.01	0	0
KOH Uptake w/r to Average				
- 1 68% average	+ 13	+ 05	- 43	22
+ 96% average	+ 21	- 53	+ 26	0
KOH Titration w/r to Average				
- 29 59 mg/gm average	-3.76	+ 59	+2 73	-1 84
+ 27 93 average	-4 00	-1 39	+3 24	-1 66
Instrumental Analysis X-Ray Diffraction— Dry				
-	Ni $Cd(OH)_2$	Ni $Cd(OH)_2$	Ni $Cd(OH)_2$	Ni $Cd(OH)_2$
+	Ni $Ni(OH)_2$ $CaCO_3$	Ni $Ni(OH)_2$	Ni $Ni(OH)_2$ $CaCO_3$	Ni $Ni(OH)_2$ $CaCO_3$
X-Ray Diffraction Discharged	$Ni(OH)_2$ Ni $Cd(OH)_2$	$Ni(OH)_2$ Ni	$Ni(OH)_2$ Ni	$Ni(OH)_2$ Ni $Cd(OH)_2$
+ As removed	$Ni(OH)_2$ Ni	$Cd(OH)_2$ $Ni(OH)_2$ Ni	Ni $(OH)_2$ Ni $CaCO_3$	$Ni(OH)_2$ Ni
Charged	$Ni(OH)_2$ Ni $Cd(OH)_2$	$Cd(OH)_2$ $Ni(OH)_2$ Ni $CaCO_3$	$Ni(OH)_2$ Ni	$Ni(OH)_2$ Ni
Overcharged	Ni	$Cd(OH)_2$ $Ni(OH)_2$ Ni	$Ni(OH)_2$ Ni	$Cd(OH)_2$ $Ni(OH)_2$ Ni
Surface Area (m^2) - 8 28 m^2 average	7 19 12 81 7 23	4 89 <3 7 14	5 93 3 30 6 82	9 82 5 74 9 70
+ 170 m^2 average	225 175	176 155	148 147	158 147
Pore Size Distribution (+ plates only), (plates B-4 & B-8)				
Total Porosity 046 cc/gm avg	054 057	033 029	049 031	.035 048
Max. Effective Pore Diam. (μ) 31 6μ average	28 29 5	40 38	42 70	43 22
Min. Effective Pore Diam (μ) 049μ average	040 045	060 < 05	049 048	048 048
Greatest Number of Pores (units)	075 (73) 075 (67)	075 (50) 075 (37)	075 (50) 075 (34)	075 (64) 075 (40)
2nd Greatest Number of Pores (units)	1 5 (40) 1 5 (30)	3 5 (30) 3 5 (35)	3 5 (45) 1 5 (27)	1 5 (30) 3 5 (30)
Metallurgical Reduction (% Active Material) 58 8% Average	56 8	51 0	57 6	58 4
Spectrochemical Analysis				
- Fe 69 ppm average	45	55	80	115
- Cu 58 ppm average	50	52	55	86
+ Fe 162 ppm average	150	180	145	210
+ Co 1 9% average	2 0	2 0	1 6	2 1
+ Zn 468 ppm average	540	310	560	460
+ Cu 60 ppm average	60	57	25	70
Differential Thermal Analysis				
- First Peak (2nd)	246	255 (319)	248 (322)	254 (319)
- Height 14 average	1	16	8	14
- Normalized Area 48 average	6	55	42	48
+ First Peak (2nd)	240 (292)	--- (306)	--- (306)	262 (296)
+ Height 25 average	7	21	23	20
+ Normalized Area 167 average	149	194	185	153
Cell Tests				
Amp hr charge in positive	5 5	---	---	1 5
Amp hr charge in negative	7.9	---	---	3 4
Oxygen amp hr recombined	2 4	---	---	1 9

* Averages in general are for 16 batteries.

** Battery had not yet failed

PAGE MISSING FROM AVAILABLE VERSION

Table 24

Group 4 Cell Comparisons

	Battery 10	Battery 11	Battery AMI 25°	Battery AMI 10°
Order of Analysis (in 16 analyses)	7	5	4	6
Cycle - Charge Discharge	C/5 for 2 5 hr C/2 to 1 0 v	C/2 for 1 hr C/2 to 1 0 v	Constant v 65 min Load - 6 amps 35 min	Constant v 65 min Load - 6 amps 35 min
Number of Cycles When Sent for Analysis 4 448 average (of 16)* To Failure 4,691 average (of 16)	3 834 3,834	5 793 5 793	5,870 5 870	6,613 6 613
Visual Inspection Cell Thickness Cell A (top-middle-bottom) Cell B (top-middle-bottom)	812 754 816 810 766 812	807 802 820 808 786 820	809 845 822 805 827 814	814 863 822 809 833 821
Notes	Separator adhesion to surface area of all negative plates (both cells) Separator was moist— least adhesion in center of cell (one cell)	Separator adhesion on outside plates— least on inside plates (both cells) Plate adhered to inside case (one cell)	Separators dry and black— outer negative plates welded to surface of case (both cells)	Adhesion of separator to negative plates (one cell) Intermittent adhesion (other cell)
Wet Chemical Analysis Plate Weights w/r to Average				
- As removed 8 00 gm average - Dry 6 81 gm average - Loss/gm 18 gm average	- 17 - 12 - 01	+ 09 - 05 + 02	- 13 - 39 + 05	- 15 - 16 0
+ As removed 9 19 gm average + Dry 8 25 gm average + Loss/gm 11 gm average	+ 12 + 12 0	+ 15 + 22 - 01	+ 67 + 55 + 01	+ 27 + 01 + 03
KOH Uptake w/r to Average - 1 68% average + 96% average	- 45 - 29	- 69 - 07	+ 25 + 36	+ 03 + 02
KOH Titration w/r to Average - 29 59 mg/gm average + 27 93 mg/gm average	-6 11 -0 83	+7 49 +3 52	+5 46 +5 99	-2 35 +8 41
Instrumental Analysis X-Ray Diffraction— Dry - +	Ni $Cd(OH)_2$ Ni $Ni(OH)_2$	Ni $Cd(OH)_2$ Ni $Ni(OH)_2$ $CaCO_3$	Ni $Cd(OH)_2$ Ni $Ni(OH)_2$ $CaCO_3$	Ni $Cd(OH)_2$ Ni $Ni(OH)_2$ $CaCO_3$
X-Ray Diffraction Discharged	Ni $Ni(OH)_2$	Ni $Ni(OH)_2$	$Ni(OH)_2$ Ni	$Cd(OH)_2$ $Ni(OH)_2$ Ni $CaCO_3$
+ As removed Charged Overcharged	Ni $Ni(OH)_2$ Ni $Ni(OH)_2$ $Ni(OH)_2$ Ni $CaCO_3$	$Ni(OH)_2$ Ni $CaCO_3$ $Ni(OH)_2$ Ni $Ni(OH)_2$ Ni	$Ni(OH)_2$ Ni $Ni(OH)_2$ Ni $Ni(OH)_2$ Ni	$Cd(OH)_2$ $Ni(OH)_2$ Ni $Ni(OH)_2$ Ni Ni
Surface Area (m^2) - 3 28 m^2 average + 170 m^2 average	10 51 6 67 9 28 173 172	8 39 4 58 8 04 145 148	7 45 9 02 9 49 163 153	16 41 17 22 14 10 170 160
Pore Size Distribution (+ plates only), (plates B-4 & B-8) Total Porosity 046 cc/gm average Max Effective Pore Diam (μ) 31 6μ average Min Effective Pore Diam (μ) 049μ average Greatest Number of Pores (units) 2nd Greatest Number of Pores (units)	041 044 39 60 < 05 < 05 075 (70) 075 (50) 16 (23) 3 5 (50) 75 (23)	028 045 27 28 < 05 < 05 075 (46) 075 (27) 3 5 (25) 3 5 (25)	049 038 30 3 2 < 05 < 05 075 (60) 075 (87) 75 (20) 1 5 (13) 75 (13)	040 051 30 18 < 05 < 05 3 5 (58) 075 (43) 075 (51) 75 (37)
Metallurgical Reduction (% Active Material) 58 8% average	61 5	65 5	66 8	55 2
Spectrochemical Analysis - Fe 69 ppm average - Cu 58 ppm average	105 52	50 100	25 55	90 40
+ Fe 162 ppm average + Co 1 9% average + Zn 468 ppm average + Cu 60 ppm average	135 1 4 500 29	165 1 8 475 30	160 2 0 450 105	155 1 5 410 35
Differential Thermal Analysis - First Peak (2nd) - Height 14 average - Normalized Area 48 average	254 (317) 11 38	255 (318) 5 11	257 (317, 191) 11 35	253 (317) 7 28
+ First Peak (2nd) + Height 25 average + Normalized Area 167 average	--- (308) 28 170	290 (313) 99 274	245 (324) 33 250	-- (317) 17 19
Cell Tests Amp hr charge in positive Amp hr charge in negative Oxygen amp hr recombined	2 8 >5 7 ---	2 6 >17 0 ---	2 7 --- ---	1 9 --- ---

* Averages in general are for 16 batteries

PAGE MISSING FROM AVAILABLE VERSION

11. Aia, M., Structure and Stoichiometry of Nickel Hydroxides in Sintered Nickel Positive Electrodes, J. Electrochemical Soc., Vol. 114, No. 5, pp. 418-423, May 1967.

12. Aia, M., private communication, February 14, 1968.

REFERENCES

1. Nickel-Cadmium Battery Test Project—Relationship Between Operation, Life and Failure Mechanism. Volume I—Experimental Design. Martin Marietta Corporation, Baltimore, Md., Report No. ER 14543, 1966.

2. Halpert, G., and Sherfey, J. M., Nickel-Cadmium Battery Test Project—Relationship Between Operation, Life, and Failure Mechanism. Volume II—Battery Test Results. GSFC Document X-735-69-24, February 1969.

3. Halpert, G., Computer Program for Analyzing Battery Performance Data. GSFC Document X-735-66-385, 1966.

4. Betz, F. E., Life Cycle Analysis, VO-6HS Cells. Gulton Industries Final Report, October 31, 1966.

5. Sloan, R. C., Analysis of Nickel and Cadmium Electrodes from Cells Submitted by Martin Marietta Corporation. ESB Final Report, July 14, 1966.

6. Salkind, A. J., Canning, H. J., and Block, M. L., The Measurement of Pore Size and Surface Area of Porous Electrodes by Nondestructive Means. Electrochemical Technology, Vol. 2, No. 9-10, pp. 254-258, September-October 1964.

7. Brunauer, S., Emmet, P. H., and Teller, E., Adsorption of Gases in Multi-Molecular Layers, Journal of the American Chemical Society, Vol. 60, pp. 309-319, February 1938.

8. Joyner, L. G., in Scientific and Industrial Glass Blowing and Laboratory Techniques, ed. by W. E. Barr and V. J. Anhorn, pp. 257-283, Instruments Publishing Co., Pittsburgh, Pa., 1949.

9. Halpert, G., A Fortran IV Program for Calculating and Plotting Surface Area and Pore Size Distribution Data Obtained by the BET-Gas Adsorption Method. GSFC Document X-735-67-505, October 1967.

10. ASTM Committee E-2, Methods for Emission Spectrochemical Analysis, Third Ed., December 1960.

6. The average surface area for a positive plate is 170 m^2/plate (3.2 m^2/cm^2 of apparent surface). The corresponding value for the negative plate is 8.28 m^2/plate (0.16 m^2/cm^2 of apparent surface).

7. The most frequently occurring pores in the positive plates are those of .075 micron diameter. The pores are 10 to 1,000 times larger while new.

8. In the cells tested, the positive electrode had lost the 4.5-ampere-hour capacity, which is defined as the criterion at which the cell is considered to have failed. This loss was generally experienced in the operational procedures used in this battery test.

ACKNOWLEDGMENTS

The author wishes to acknowledge those who assisted with the analysis tests: J. Marello of Martin Marietta Corporation, Fred Betz and Karl Preusse of Gulton Industries, Richard Sloan of the ESB Research Center, and J. M. Sherfey and W. R. Campbell of Goddard Space Flight Center.

The differential thermograms are a means of determining the relative amounts of active material in the charged or discharged phase. As with the other tests, the variation from plate to plate made it difficult to compare the materials of one battery with those of another.

Cell Tests

It is interesting to note that the positive electrode failed first in every instance when the cells were discharged to second failure. The excess charge left in the negative electrode was a minimum of 3.4 ampere-hours. As proof of this amount, the equivalent capacity of oxygen recombined in a cell varied between 2.2 and 7.2 ampere-hours. It is apparent that in many of these instances it was the positive electrode that performed poorly. This was the cause of a loss in capacity greater than 4.5 ampere-hours for Batteries 0, 1, 2, 4, 7, and 9. The capacity in the negative electrode exceeded 4.0 ampere-hours with the exception of Battery 9, for which it was 3.4 ampere-hours.

CONCLUSIONS

A number of conclusions can be drawn from the results of the visual examination, wet analysis, instrumental analysis, and cell tests. These conclusions are listed below.

1. The major mode of failure appears to be the drying-out of the separator and the adhesion of the separator to the negative plate. Growth of negative materials into the separator is also present.

2. Negative plates absorb almost twice as much electrolyte as do positive plates.

3. Cells generally degrade in the above manner irrespective of the type of operation to which they are subjected. There are exceptions, such as high-rate discharge, which causes plate blistering in addition to the general degradation.

4. There is considerable variation between plates in the same cell as well as between cells from different batteries, so that singling out a chemical or physical characteristic leading to failure is a difficult task.

5. The appearance of carbonates, both calcium and cadmium, on the surface of the plates is either a cause of or a consequence of the degradation process. Other substances such as silver, zinc, copper, and iron should be kept out of the cell.

oxidation of the separator, which after much cycling had become dry, was warm during oxygen evolution, and was in the presence of oxygen, a situation which is conducive to hydrolysis and oxidation of nylon. Cadmium hydroxide was found in three instances on the surface of the positive plate, a condition giving some evidence of high-resistance shorting between plates in some of the cells. It was found also in the separator, so manifestly the $Cd(OH)_2$ worked its way from the negative to the positive plate.

Of all the batteries, only AMF 10° plate materials exhibited a negative surface area significantly higher than the average. This difference may be indicative of the low-temperature operation. The positive electrodes of the control battery had surface areas of 190 square meters, which was also significantly greater than for the others. Since high surface area is desirable and a characteristic of a good battery, the control battery, which had been given only conditioning cycles, was in the desirable condition.

There is also a significant difference between the 146.5-square-meter positive plates of Battery 11 (C/2 charge for 1 hour) and the 172.5-square-meter positive plates of Battery 10 (C/5 charge for 2.5 hours). A further difference between the two is the length of operation: 5,793 cycles for Battery 11 and 3,834 cycles for Battery 10.

The pore size distribution data for the batteries lead to only one conclusive point, namely, that the most frequent pore size for all the batteries after cycling for prolonged periods, with the exception of the control battery, is .075 microns. The chief pore sizes for the two plates of the control battery are .75 and 75 microns. The larger size is consistent with the larger surface area for these plates.

An increase in silver content was noted in the same order as that in which the batteries were analyzed. This increase was probably due to the silver from the braze in the ceramic-to-metal seal. Only one short due to silver migration was found, and it was in Battery 5, which failed within a few hundred cycles. Some iron was found in the plates, it probably had come from the perforated steel base of each plate. The copper and zinc found were probably due to the brass valves attached to the pressure gauge, or may have been due to the separator. Even though a given cell had no gauge, a brass fitting was used on every cell before completing the sealing process. No significant failure due to the impurities was found, but for future aerospace applications and especially for long-term missions an effort should be made to eliminate impurities from the cells.

negative plate weight loss accompanying the washing and drying of the plates was significantly below the average. This result, together with the fact that the separators from these cells were moist and not attached to the negative plate, is probably an indication that, in the instance of the control battery, in which the cells were not excessively cycled, the electrolyte remained in the separator rather than migrate into the plates. The longer the cells were operated, the greater the movement of electrolyte from the separator into the plates. This is consistent with the results of the KOH titration and KOH uptake tests, which accounted for concentration of KOH in the plates and dryness of the plate materials.

In the instance of Battery 2, although operating time (number of cycles) was short, the heat generated during the high-rate discharge probably expedited the transfer of the electrolyte to the plates. The results for the AMF 25° cells support this position from the opposite direction. The plates from these cells had the highest weight when removed and the greatest loss in weight when washed and dried. The results given in Figure 7 indicate that the AMF 25° cell results are also sufficiently non-random to be considered a real effect. The AMF 25° battery was operated at 58% depth of discharge for 5,870 cycles and discharged at the C rate, which was the most severe operation of all the cells.

Instrumental Analysis

Of significance in the X-ray diffraction measurement is the fact that calcium carbonate appeared as a major constituent on the surface of most positive plates. This substance, which increases resistance and polarization, appeared to form over the longer operating periods, i.e., in the positive plates of Batteries 0 and 2 and the control battery no $CaCO_3$ was present but it was found in Battery 1, which was operated for a longer time. In another instance, it was found as a minor constituent (Battery 8A); six months later, it was found in a cell from the same battery (8B) as a major constituent. The $CaCO_3$ was found to be on the surface of the positive plates only. An X-ray pattern of a pulverized plate from Battery 4 exhibited no peaks attributed to the $CaCO_3$, because the $CaCO_3$ was concentrated at the surface but when mixed with the bulk material became a very small percentage. Cadmium carbonate ($CdCO_3$) was found on the surface of most negative plates as a minor constituent. The appearance of $CaCO_3$ and $CdCO_3$ on the surface is significant because they become a mode for degradation. The question arises of how these substances entered the cell in the first place; the cells were all sealed and epoxied. Calcium may have entered the cell as a constituent of the electrolyte or of the water used to dilute the electrolyte. The carbonate may have been due to the

~~1 SEP 70 N~~ ~~Donald M Bowdish~~ 354/33/24994 300 I8

~~8 DEC 70 N R Stengel E454/101/26416~~

~~9 SEP 70 N B K Ruthbaumkas E454/106/26416~~

~~A D Taylor E454/106/21197~~

~~B K Ruthbaumkas E454/106/26416~~

~~9-6-74 VC Mueller E454/106-5/26~~ 811 20 JAN 75 (B)